M.TECH [POWER SYSTEMS] [MANSI TRIPATHI] 2022

MODELLING AND ANALYSIS OF FLYBACK CONVERTER

A Dissertation

Submitted in partial fulfillment of

the requirements for the degree of

Master of Technology

In

Power Systems

By

[Mansi Tripathi]

(Roll No. 2K20/PSY/11)

Under the Supervision of

[Prof. Dheeraj Joshi]

DEPARTMENT OF ELECTRICAL ENGINEERING

DELHI TECHNOLOGICAL UNIVERSITY

(Formerly Delhi College of Engineering)

Bawana Road, Delhi-110042

June 22

DEPARTMENT OF ELECTRICAL ENGINEERING
DELHI TECHNOLOGICAL UNIVERSITY
(Formerly Delhi College of Engineering)
Bawana Road, Delhi-110042

CANDIDATE'S DECLARATION

I, **(Mansi Tripathi)**, having roll no. **2K20/PSY/11** of M. Tech (**Power Systems**), hereby declare that the project Dissertation titled "**Modelling and Analysis of Flyback Converter**" which is submitted by me to the Department of Electrical Engineering, Delhi Technological University, Delhi in partial fulfilment of the requirement for the award of the degree of Master of Technology, is original and not copied from any source without proper citation. Work has not earlier formed the basis for the award of any Degree, Diploma Associateship, Fellowship or other similar title or recognition.

Place: Delhi
Date: 7-Jun-22

_____
Mansi Tripathi
(2K20/PSY/11)

DEPARTMENT OF ELECTRICAL ENGINEERING
DELHI TECHNOLOGICAL UNIVERSITY
(Formerly Delhi College of Engineering)
Bawana Road, Delhi-110042

CERTIFICATE

I hereby certify that the Project Dissertation titled "**Modelling and Analysis of Flyback Converter**" which is submitted by [Mansi Tripathi], 2K20/PSY/11 of Electrical Engineering Department, Delhi Technological University, Delhi in partial fulfilment of the requirement for the award of the degree of Master of Technology, is a record of the project work carried out by the scholar under my supervision. To the best of my knowledge this work has not been submitted in part or full for any Degree or Diploma to this University or somewhere else.

Place: Delhi
Date: 7-Jun-22

_____
(Prof. Dheeraj Joshi)
SUPERVISOR

ACKNOWLEGDEMENT

I would like to thank Prof. Dheeraj Joshi for his numerous discussions and suggestions to explore various aspect of problem statement. Moreover, I appreciate the feedback given by faculties during the mid-year project evaluation.

I would like to acknowledge Prof. Uma Nangia, Head of the Dept. of Electrical Engineering, DTU, Delhi for extending their support during Course of this study.

Mansi Tripathi

DTU, Delhi

31-05-2022

ABSTRACT

In late 60's demand made by space programs led to the development of power supplies that are highly reliable, efficient, light weight and small. The innovative ideas of the engineer's usher in the era of modern power electronics and switch mode power supplies came into existence. Design and optimization of dc-dc converter which offers high efficiency, small converters with isolation transformers can have multiple outputs of various magnitudes and polarities. The regulated power supply of this type has a wide application such as digital systems, in TVs instrumentation system, in industry automation etc., where in a low voltage, high current power supply with low output ripple and fast transient response are essential.

A new model has been proposed for the analysis of Flyback converter with coupled inductance. The model transforms any dynamic circuit into a resistive circuit. The method is based on the discrete equivalent circuit approach. In this way, a fully resistive flyback circuit has been obtained with discrete equivalents of coupled inductor and capacitor. The proposed model makes the analysis easier.

CONTENT

LIST OF FIGURES

LIST OF SYMBOLS AND ABBREVIATIONS

DCM	Discontinuous Conduction Mode
PID	Proportional-Integral-derivative
MNA	Modified Nodal Approach
CCM	Continuous Conduction Mode
EN/UV	Enable / Under Voltage
BP/M	Bypass / Multifunction
D / S	Drain / Source
PWM	Pulse Width Modulation
SISO	Single Input and Single Output
LTI	Linear Time Invariant
MMC	Modular Multilevel Converter

CHAPTER 1

1. INTRODUCTION

Power Electronics Systems have numerous applications such as high voltage DC transmission systems (HVDC), flexible AC transmission system (FACTS) devices and AC-DC motor drives. However, some difficulties are encountered in the analysis of both the electrical networks and power electronic circuit. The method by which circuit equations are formulated is of key importance to a computer-aided circuit analysis and design program for integrated circuits. The nodal approach for formulating circuit equations is a classical method, however it treats voltage sources inefficiently and is incapable of including dependent elements. Another disadvantage of the nodal method is that branch currents are not accurately or conveniently obtained. We therefore go for self-consistent modifications to the nodal method and the formulation is called modified nodal analysis (MNA). Further the use of MNA equations along with the companion model of coupled inductor and capacitor provide us with the discrete model of the flyback converter. Recent advances in digital control of high-frequency switched-mode power converters have renewed the interest in discrete-time modelling techniques as more natural and more accurate representations of the converter dynamics when controlled digitally. Discrete-time modelling aims at describing the dynamics of the sampled converter waveforms, with no averaging step involved in the process.

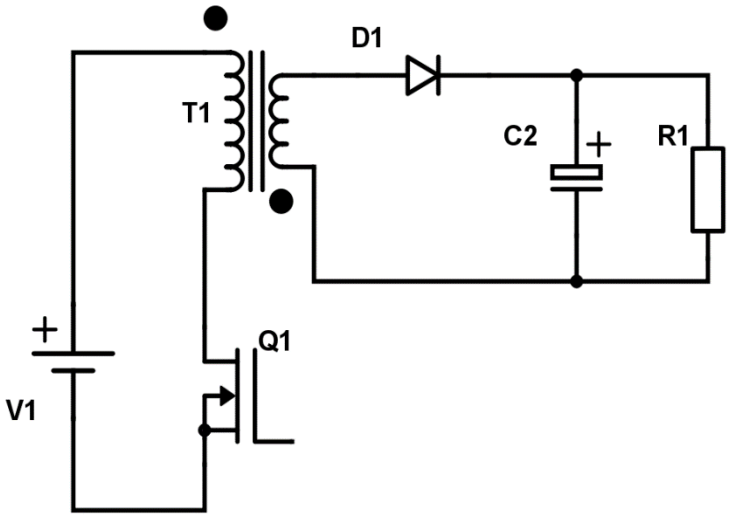

Fig. 1 : Flyback Converter Topology

Analysing and designing of DC–DC converters which offers high efficiency, small converters with the implementation of isolation transformer can have numerous outputs of various magnitude and polarities. Flyback converter (Fig. 1) is a DC/DC converter which is a advance version of buck-boost converter where a transformer for galvanic isolation between input and output is placed by removing inductor. Designing a sliding mode controller must satisfy the robustness and performance criteria so that as the disturbance occurs in the plant must be handled with proper feedback. These models are broadly used to study the static and dynamic features of the converters as well as to design their control systems to reach specific regulation features.

Basic working and operation of buck boost converter is explained in Section 1.1 which advances to working and operation of flyback converter in Section 1.2.

1.1. BUCK BOOST CONVERTER

A DC/DC converter is used usually to transfer DC voltage at one level to another level where input voltage is chosen by different voltage source. Buck boost converter shown in (Fig. 2), is capable of generating an output voltage higher or lower value than the input voltage and has property to step up or step down the output voltage. Its voltage gain equation is stated as

$$\frac{V_{out}}{V_{in}} = \frac{D}{1-D} \qquad 1.1$$

V_{out}: $Output\ voltage\ across\ capacitor\ C1$

V_{in}: $Input\ source\ voltage\ V1$

D: $duty\ cycle\ of\ switching\ pulse$

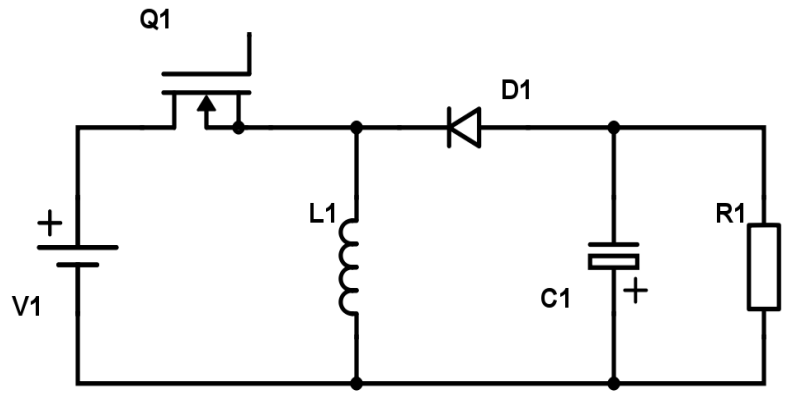

Fig. 2 : Buck Boost Converter Design.

1.1.1. OPERATION

A buck boost converter has the same configuration as that of flyback converter but there is no transformer. It consists of a switch (Q1), a voltage source V1, an inductor L1, a power diode D1, a capacitor C1 and a resistive load R1 working in continuous conduction mode (CCM) for operation. Assuming the steady state condition capacitor is initially charged having V_{out} voltage across it and a finite current flow through the inductor. Let us consider that the switch Q1 is ON, so input dc voltage V1 charges the inductor L1 magnetically as the diode D1 is reversed biased. This leads to surge in inductor current expressed by

$$V = L * \left(\frac{di}{dt}\right) \quad 1.2$$

V: $Voltage\ across\ inductor\ L$

L: $Value\ of\ inductance\ in\ mH$

i: $Inductor\ current\ in\ A$

And when the switch Q1 is switched OFF, the current in the inductor L1 is going to transfer energy to the capacitor C1 in the same direction, making diode D1 forward bias and starts conducting according to Faradays Law of Electromagnetic Induction. The capacitor will charge in opposite direction so the output will be inverted.

To derive voltage gain expression, we can use the condition that average voltage across inductor ought to be equal to zero.

During ON state,

$$V_{L1} = V_{in}$$

and during OFF state,

$$V_{L1} = V_{out}$$

Applying average voltage conditions, we get

$$V_{in} * D * T - V_{out} * (1 - D) * T = 0 \quad 1.3$$

$$\frac{V_{out}}{V_{in}} = \frac{D}{1-D} \quad 1.4$$

T: $Time\ period\ of\ switching\ pulse$

So, the final Equation 1.4 represents the voltage expression for buck boost converter.

1.2. FLYBACK CONVERTER

It is known that flyback converter (Fig. 3) is an isolated converter by replacing inductor in buck boost converter with a high frequency transformer.

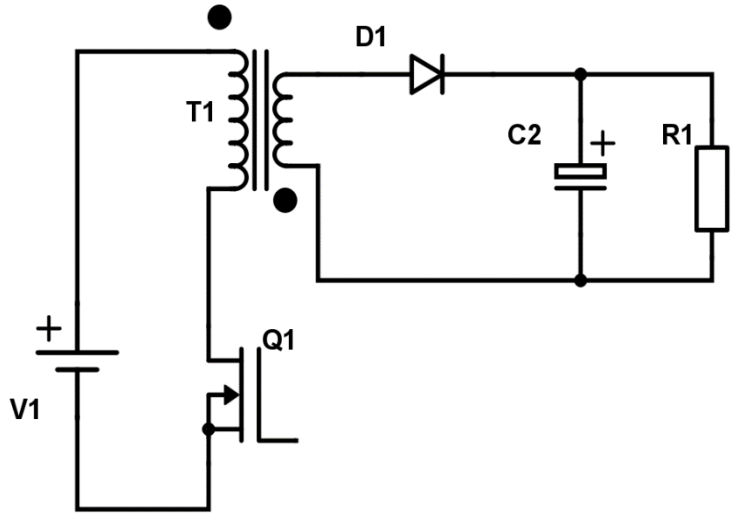

Fig. 3 : Basic Flyback Converter.

Voltage gain expression for the flyback converter is described as

$$\frac{V_{out}}{V_{in}} = \frac{N_2}{N_1} * \frac{D}{1-D} \qquad 1.5$$

N_1: $Number\ of\ turns\ on\ the\ transformer\ primary\ side\ in\ converter$

N_2: $Number\ of\ turns\ on\ the\ transformer\ secondary\ side\ in\ converter$

The simplified working is explained in the next section.

1.2.1. OPERATION

In any converter there are basic two states of a switch, which are used in expressing the voltage gain equation. We will be following the same procedure as in case of buck boost converter.

During the switch Q1 is in ON state, the current build up in the primary side of the transformer T1 as the input DC voltage power the primary side. In result to that energy gets stored in the magnetising inductance L_m of transformer. Diode D1 will be reversed bias due to dot polarity of the transformer T1, so secondary side will be open

circuited, and it will not conduct. During this condition, capacitor (C_1) provide current to the load.

And when the switch Q1 is switched OFF, as per the dot polarity of the transformer the current in the inductor Lm is going to transfer energy to the capacitor C1 in the same direction, making diode D1 forward bias on the secondary side and starts conducting according to Faradays Law of Electromagnetic Induction.

Fig. 4 demonstrates the voltage and current waveform for ON and OFF state of switch (Q1).

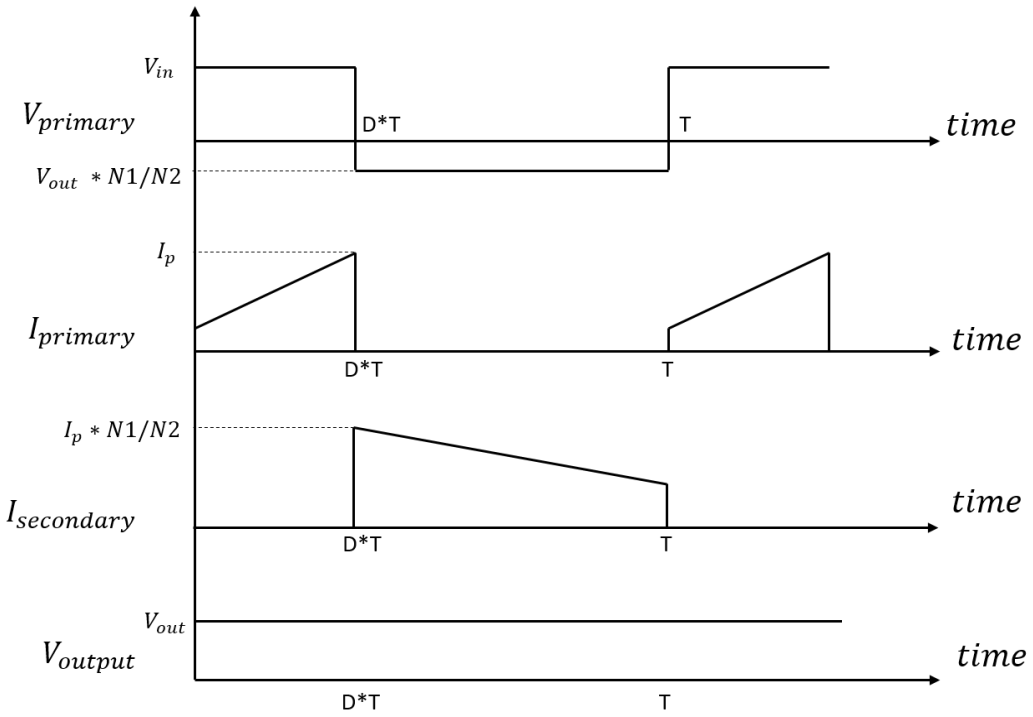

Fig. 4 : Voltages and Currents waveform for the switching of converter.

I_p in the plot signify current (peak current) through the primary side of the transformer (T_1). To find voltage gain expression, we need to apply average voltage criteria on the primary side of transformer (T1) to obtain:

$$V_{in} * D \ * \ T - V_{out} * \frac{N_1}{N_2} * (1 - D) * T = 0 \qquad 1.6$$

$$\frac{V_{out}}{V_{in}} = \frac{N_2}{N_1} * \frac{D}{1-D} \qquad 1.7$$

So, the equation 1.7 represents the voltage gain expression of Flyback converter.

1.2.2. AVERAGE VALUE MODELLING OF FLYBACK CONVERTER

The averaged-value modelling, where the effects of fast switching are "averaged" over a switching interval, is most frequently applied when investigating power-electronics-based systems. Continuous large-signal models are typically non-linear and can be linearized around a desired operating point. Averaged models of dc-dc converters overture several advantages. These advantages are:

i) straightforward approach in decisive local transfer-functions;
ii) faster simulation of large-signal system-level transients; and
iii) use of general-purpose simulators to linearize converters for designing the feedback controllers.

A typical switched-inductor dc-dc converter can operate in two modes. One is the Continuous Conduction Mode (CCM) in which inductor current never falls to zero. The second mode is Discontinuous Conduction Mode (DCM) allowing inductor current to turn out to be zero for a portion of switching period. The DCM typically occurs at light loads and differs from CCM. This mode results into three different switched networks over one switching.

Average value models may be considered as resulting system of equations or by derivation methodology (sampled data modelling, circuit averaging, state-space averaging). The full-order as well as reduced-order models can be obtained by averaging approaches including sampled data modelling, state space averaging or circuit averaging. The conventional reduced order models express the discontinuous variable as a dependent variable, thus eliminate its dynamic from the state equations.

State-space averaging is built on the conventional averaging theory and involves operation of state-space calculations of a converter system. First, a state-space representation of converter is obtained for each topology and subinterval. Then, the obtained piece-wise linear equations are weighted by the corresponding time subinterval length and added together. State-space averaging has been demonstrated to be an effective method to analyse PWM converters. Analytical averaging, however, is based on so-called small-ripple approximation.

CHAPTER 2

2. STATE SPACE AVERAGING AND SMALL SIGNAL ANALYSIS AC MODEL WITH BASIC PARASITICS IN CONTINOUS CONDUCTION MODE

State space averaging approximates the switching converter as a continuous linear system. In state space average modelling, the switching circuit is split into two (Continuous Conduction Mode) or three (Discontinuous Conduction Mode) different structure. Base of modern control theory is the state-space modelling of dynamical systems. The state-space averaging method is else identical to the technique of deriving the small-signal ac model. To derive the small-signal averaged calculations of the PWM switching converters we make use of this explanation of state-space averaging technique. An advantage of the state-space averaging modelling is its outcomes: a small-signal averaged model that can constantly be found, on condition that the state equations of the novel converter can be inscribed.

A diagram of second order flyback converter by means of basic parasitics is shown in Fig. 5a. Here, *n* is the transformer (N_1/N_2) turns ratio.

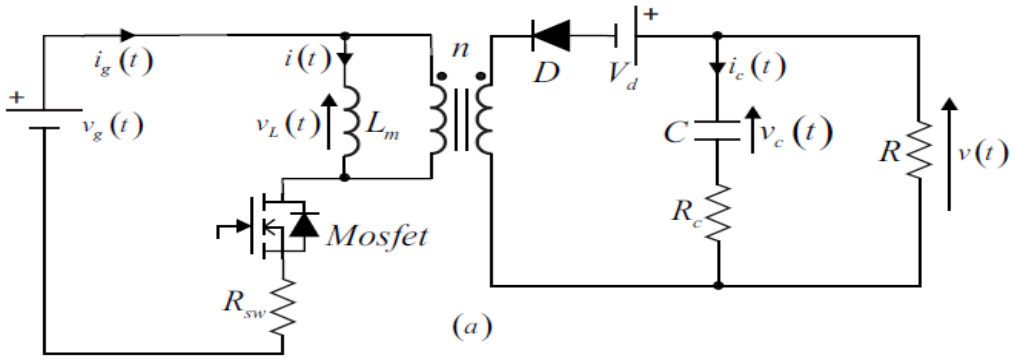

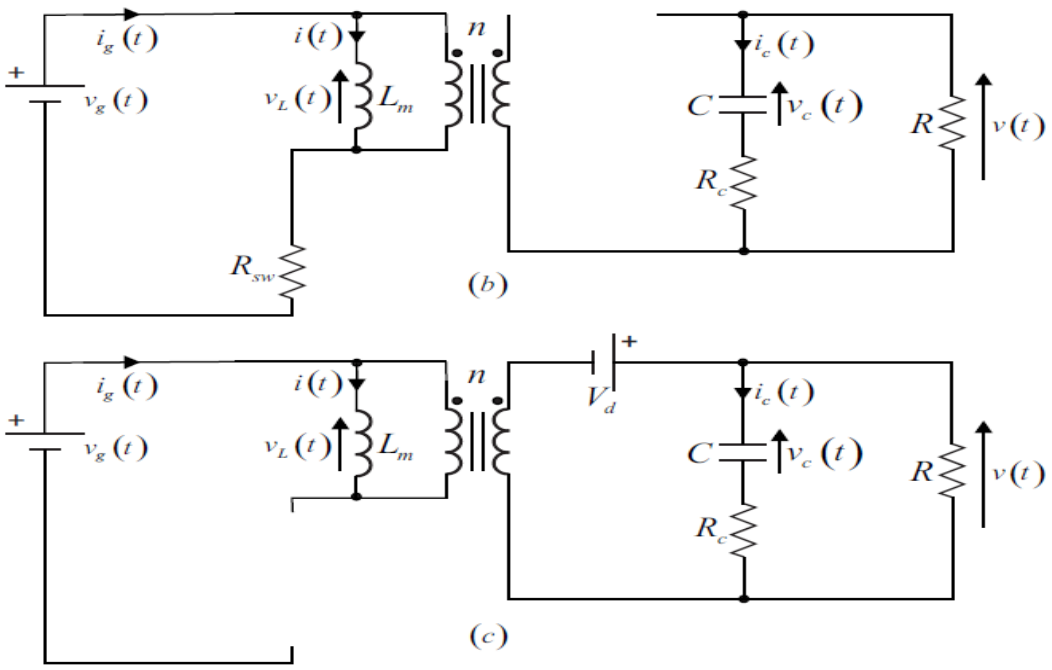

Fig. 5 : (a) Flyback converter (Second order) with practical parasites; (b) Subinterval 1 of circuit (c) Subinterval 2 of circuit.

Through the first subinterval, when the MOSFET is switched ON and the diode is OFF, the circuit lessens to Fig. 5b. For this instant, the inductor voltage $v_L(t)$, converter input current $i_g(t)$, converter output voltage v(t), and capacitor current $i_c(t)$.

$$v_L(t) = v_g(t) - R_{sw} i_g(t) \quad 2.1$$

$$i_g(t) = i(t) \quad 2.2$$

$$v(t) = \frac{v_c(t)R}{R+R_c} \quad 2.3$$

$$i_c(t) = -\frac{v_c(t)}{R+R_c} \quad 2.4$$

During the second subinterval, while the MOSFET is off besides the diode conducts, the circuit decreases to Fig. 5c. For this instant, the inductor voltage $v_L(t)$, converter output voltage $v(t)$, capacitor current $i_c(t)$, and converter input current $i_g(t)$.

$$v_L(t) = (v_c(t) - i_c(t)R_c - V_d)n \quad 2.5$$

$$v(t) = v_c(t) - i_c(t)R_c \quad 2.6$$

$$i_c(t) = -\left(i(t)n + \frac{v(t)}{R}\right) \quad 2.7$$

$$i_g(t) = 0 \tag{2.8}$$

The average inductor voltage can be expressed by averaging the subintervals over one whole switching period. The outcome is

$$\begin{aligned}\langle v_L(t)\rangle_{T_s} &= \langle v_g(t)\rangle_{T_s} d_1(t) - R_{sw}\langle i_g(t)\rangle_{T_s} d_1(t) \\ &+\langle v_c(t)\rangle_{T_s} n d_2(t) - \langle i_c(t)\rangle_{T_s} n R_c d_2(t) - V_d n d_2(t)\end{aligned} \tag{2.9}$$

This primes to the subsequent calculation for the average inductor current

$$\begin{aligned}L_m \frac{d\langle i(t)\rangle_{T_s}}{dt} &= \langle v_g(t)\rangle_{T_s} d_1(t) - R_{sw}\langle i_g(t)\rangle_{T_s} d_1(t) \\ &+\langle v_c(t)\rangle_{T_s} n d_2(t) - \langle i_c(t)\rangle_{T_s} R_c n d_2(t) - V_d n d_2(t)\end{aligned} \tag{2.10}$$

The average capacitor current now can be initiated by averaging the subintervals concluded over one switching period, which fallouts to be

$$\langle i_c(t)\rangle_{T_s} = -\frac{\langle v_c(t)\rangle_{T_s}}{R+R_c} d_1(t) - \langle i(t)\rangle_{T_s} n d_2(t) - \frac{\langle v(t)\rangle_{T_s}}{R} d_2(t) \tag{2.11}$$

This primes to the subsequent calculation for the average capacitor voltage

$$C\frac{d\langle v_c(t)\rangle_{T_s}}{dt} = -\frac{\langle v_c(t)\rangle_{T_s}}{R+R_c} d_1(t) - \langle i(t)\rangle_{T_s} n d_2(t) - \frac{\langle v(t)\rangle_{T_s}}{R} d_2(t) \tag{2.12}$$

The converter output voltage now can be expressed by averaging subintervals over one switching period, which expressed as

$$\langle v(t)\rangle_{T_s} = \frac{\langle v_c(t)\rangle_{T_s} R}{R+R_c} d_1(t) + \langle v_c(t)\rangle_{T_s} d_2(t) - \langle i_c(t)\rangle_{T_s} R_c d_2(t) \tag{2.13}$$

The input current of the converter can now be expressed by averaging the subintervals over one switching period, resulting

$$\langle i_g(t)\rangle_{T_s} = \langle i(t)\rangle_{T_s} d_1(t) + 0 \tag{2.14}$$

Where duty cycles are denoted by $d_1(t)$ and $d_2(t)$ respectively for the particular sub-intervals. The equations (2.10), (2.12), (2.13) and (2.14) are nonlinear differential equations. The equations are perturbed and linearized to develop the converter small-signal ac model. Statement made that the converter duty cycle $d_1(t)$ and input voltage $v_g(t)$ can be expressed as dormant values plus minor ac variations, as expressed

$$d_1(t) = D_1 + \hat{d}_1(t) \tag{2.15}$$

$$\langle v_g(t)\rangle_{T_s} = V_g + \hat{v}_g(t) \tag{2.16}$$

In response to these inputs, and later all transients have decayed, the averaged converter waveforms can be stated as quiescent values plus small ac variations as

$$\langle i(t)\rangle_{T_s} = I + \hat{i}(t) \tag{2.17}$$

$$\langle i_g(t)\rangle_{T_s} = I_g + \hat{i}_g(t) \tag{2.18}$$

$$\langle v_c(t)\rangle_{T_s} = V_c + \hat{v}_c(t) \tag{2.19}$$

$$\langle i_c(t)\rangle_{T_s} = I_c + \hat{i}_c(t) \tag{2.20}$$

$$\langle v(t)\rangle_{T_s} = V + \hat{v}(t) \tag{2.21}$$

the large-signal averaged inductor, (2.10), converts to with these substitution is expressed below,

$$\begin{aligned} L_m \frac{d\left(I+\hat{i}(t)\right)}{dt} &= \left(V_g + \hat{v}_g(t)\right)\left(D_1 + \hat{d}_1(t)\right) - R_{sw}\left(I_g + \hat{i}_g(t)\right)\left(D_1 + \hat{d}_1(t)\right) \\ &+ \left(V_c + \hat{v}_c(t)\right)n\left(D_2 - \hat{d}_1(t)\right) - \left(I_c + \hat{i}_c(t)\right)R_c n\left(D_2 - \hat{d}_1(t)\right) \\ &- V_d n\left(D_2 - \hat{d}_1(t)\right) \end{aligned} \tag{2.22}$$

After simplification, we find

$$\begin{aligned} L_m\left(\frac{dI}{dt} + \frac{d\hat{i}(t)}{dt}\right) &= \left(V_g D_1 - R_{sw} I_g D_1 + V_c n D_2 - I_c R_c n D_2 - V_d n D_2\right) \\ &+ \begin{pmatrix} V_g \hat{d}_1(t) + \hat{v}_g(t) D_1 - R_{sw} I_g \hat{d}_1(t) - R_{sw}\hat{i}_g(t) D_1 - V_c n \hat{d}_1(t) \\ + \hat{v}_c(t) n D_2 + I_c R_c n \hat{d}_1(t) - \hat{i}_c(t) R_c n D_2 + V_d n \hat{d}_1(t) \end{pmatrix} \\ &+ \begin{pmatrix} \hat{v}_g(t)\hat{d}_1(t) - R_{sw}\hat{i}_g(t)\hat{d}_1(t) - \hat{v}_c(t) n \hat{d}_1(t) \\ + \hat{i}_c(t) n R_c \hat{d}_1(t) + V_d n \hat{d}_1(t) \end{pmatrix} \end{aligned} \tag{2.23}$$

Certainly, from the above equation, three different types of terms are observed. Firstly, the dc term contains no time-varying quantities. The first order ac terms are linear functions of the ac variations in the circuit. Though the second order ac terms are the

product of the ac variations. At this point, it is assumed that the ac variations are minor in value equated to the dc quiescent values,

$$\begin{aligned} |\hat{v}_g(t)| &\ll |V_g| \\ |\hat{d}_1(t)| &\ll |D_1| \\ |\hat{i}_g(t)| &\ll |I_g| \\ |\hat{i}(t)| &\ll |I| \\ |\hat{v}_c(t)| &\ll |V_c| \\ |\hat{i}_c(t)| &<< |I_c| \\ |\hat{v}(t)| &<< |V| \end{aligned} \qquad 2.24$$

As soon as the small signal estimate (2.24) are fulfilled, then the second-order terms are smaller in magnitude in compare to the first-order terms. Hence be neglected. The dc terms essential follow

$$0 = V_g D_1 - R_{sw} I_g D_1 + V_c n D_2 - I_c n R_c D_2 - V_d n D_2 \qquad 2.25$$

The first order terms essentially follow

$$\begin{aligned} L_m \frac{d\hat{i}(t)}{dt} = \; & V_g \hat{d}_1(t) + \hat{v}_g(t) D_1 - R_{sw} I_g \hat{d}_1(t) - R_{sw} \hat{i}_g(t) D_1 - V_c n \hat{d}_1(t) \\ & + \hat{v}_c(t) n D_2 + I_c R_c n \hat{d}_1(t) - \hat{i}_c(t) R_c n D_2 + V_d n \hat{d}_1(t) \end{aligned} \qquad 2.26$$

Above equation 2.26 is a linear expression that describes ac dissimilarities in the inductor current.

On substituting equations (2.15)-(2.21) into (2.12), we get

$$\begin{aligned} C \frac{d(V_c + \hat{v}_c(t))}{dt} = \; & -\frac{(V_c + \hat{v}_c(t))}{R + R_c}(D_1 + \hat{d}_1(t)) - (I + \hat{i}(t)) n (D_2 - \hat{d}_1(t)) \\ & - \frac{(V + \hat{v}(t))}{R}(D_2 - \hat{d}_1(t)) \end{aligned} \qquad 2.27$$

Simplifying and sorting the above equation 2.27, we find

$$C\left(\frac{dV_c}{dt}+\frac{d\hat{v}_c(t)}{dt}\right)=\left(-\frac{V_cD_1}{R+R_c}-\mathrm{In}D_2-\frac{VD_2}{R}\right)$$
$$+\left(-\frac{V_c\hat{d}_1(t)}{R+R_c}-\frac{\hat{v}_c(t)D_1}{R+R_c}+\mathrm{In}\hat{d}_1(t)-\hat{i}(t)nD_2+\frac{V\hat{d}_1(t)}{R}-\frac{\hat{v}(t)D_2}{R}\right) \quad 2.28$$
$$+\left(-\frac{\hat{v}_c(t)\hat{d}_1(t)}{R+R_c}+\hat{i}(t)n\hat{d}_1(t)+\frac{\hat{v}(t)\hat{d}_1(t)}{R}\right)$$

Here again we exclude the second-order terms in equation (2.28). The dc terms of equation (2.28) must satisfy

$$0=-\frac{V_cD_1}{R+R_c}-\mathrm{In}\,D_2-\frac{VD_2}{R} \quad 2.29$$

The first-order ac terms of (2.28) lead to the following small-signal for the ac capacitor voltage

$$C\frac{d\hat{v}_c(t)}{dt}=-\frac{V_c\hat{d}_1(t)}{R+R_c}-\frac{\hat{v}_c(t)D_1}{R+R_c}+\mathrm{In}\,\hat{d}_1(t)-\hat{i}(t)nD_2+\frac{V\hat{d}_1(t)}{R}-\frac{\hat{v}(t)D_2}{R} \quad 2.30$$

Substitution of (2.15) -(2.21) into (2.13) leads to

$$(V+\hat{v}(t))=\frac{(V_c+\hat{v}_c(t))}{R+R_c}R(D_1+\hat{d}_1(t))+(V_c+\hat{v}_c(t))(D_2-\hat{d}_1(t))$$
$$-(I_c+\hat{i}_c(t))R_c(D_2-\hat{d}_1(t)) \quad 2.31$$

On multiplying and sorting this equation, we get

$$(V+\hat{v}(t))=\left(\frac{V_cD_1R}{R+R_c}+V_cD_2-I_cR_cD_2\right)$$
$$+\left(\begin{array}{c}\frac{V_cR\hat{d}_1(t)}{R+R_c}+\frac{\hat{v}_c(t)RD_1}{R+R_c}-V_c\hat{d}_1(t)+\hat{v}_c(t)D_2\\ +I_cR_c\hat{d}_1(t)-\hat{i}_c(t)R_cD_2\end{array}\right) \quad 2.32$$
$$+\left(\frac{\hat{v}_c(t)R\hat{d}_1(t)}{R+R_c}-\hat{v}_c(t)\hat{d}_1(t)+\hat{i}_c(t)R_c\hat{d}_1(t)\right)$$

The dc term must satisfy

$$V=\frac{V_cD_1R}{R+R}+V_cD_2-I_cR_cD_2 \quad 2.33$$

the second-order terms in equation (2.32) is excluded and parting the following linearized ac expression

$$\hat{v}(t) = \frac{V_c R \hat{d}_1(t)}{R+R_c} + \frac{\hat{v}_c(t) R D_1}{R+R_c} - V_c \hat{d}_1(t) + \hat{v}_c(t) D_2 + I_c R_c \hat{d}_1(t) - \hat{i}_c(t) R_c D_2 \qquad 2.34$$

Substituting equations (2.15)-(2.21) into (2.14) leads to

$$I_g + \hat{i}_g(t) = (I + \hat{i}(t))(D_1 + \hat{d}_1(t)) \qquad 2.35$$

On multiplying and simplifying this equation, we get

$$I_g + \hat{i}_g(t) = (ID_1) + (I\hat{d}_1(t) + \hat{i}(t)D_1) + (\hat{i}(t)\hat{d}_1(t)) \qquad 2.36$$

DC term must satisfy

$$I_g = ID_1 \qquad 2.37$$

the second-order terms in equation (2.36) is excluded and parting the subsequent linearized ac expression

$$\hat{i}_g(t) = I\hat{d}_1(t) + \hat{i}(t)D_1 \qquad 2.38$$

The equations of the quiescent values, (2.25), (2.29), (2.33), and (2.37) are collected below as

$$\left.\begin{aligned} 0 &= V_g D_1 - R_{sw} I_g D_1 + V_c n D_2 - I_c R_c n D_2 - V_d n D_2 \\ 0 &= -\frac{V_c D_1}{R+R_c} - \ln D_2 - \frac{V D_2}{R} \\ V &= \frac{V_c D_1 R}{R+R_c} + V_c D_2 - I_c R_c D_2 \\ I_g &= ID_1 \end{aligned}\right\} \qquad 2.39$$

For supposed quiescent values of the diode voltage drops V_d, input voltage V_g, and the duty cycle D_1, the system (2.39) can be estimated to find the quiescent inductor current I, input current I_g, output voltage V, capacitor current I_c, and capacitor voltage V_c. However, in this problem there are 5 variables but there are only 4 equations. The fifth equation can be the following

$$V = V_c - I_c R_c \qquad 2.40$$

The outcomes of the expression are then introduced into the small-signal ac model.

The small signal ac model, (2.26), (2.30), (2.34), and (2.38), is summarized below

$$\begin{aligned}
L_m \frac{\hat{di}(t)}{dt} &= V_g \hat{d}_1(t) + \hat{v}_g(t)D_1 - R_{sw} I_g \hat{d}_1(t) - R_{sw}\hat{i}_g(t)D_1 - V_c n\hat{d}_1(t) \\
&\quad + \hat{v}_c(t)nD_2 + I_c R_c n\hat{d}_1(t) - \hat{i}_c(t)R_c nD_2 + V_d n\hat{d}_1(t) \\
C\frac{\hat{dv}_c(t)}{dt} &= -\frac{V_c \hat{d}_1(t)}{R+R_c} - \frac{\hat{v}_c(t)D_1}{R+R_c} + \mathrm{In}\,\hat{d}_1(t) - \hat{i}(t)nD_2 + \frac{V\hat{d}_1(t)}{R} - \frac{\hat{v}(t)D_2}{R} \\
\hat{v}(t) &= \frac{V_c R\hat{d}_1(t)}{R+R_c} + \frac{\hat{v}_c(t)RD_1}{R+R_c} - V_c\hat{d}_1(t) + \hat{v}_c(t)D_2 + I_c R_c\hat{d}_1(t) - \hat{i}_c(t)R_c D_2 \\
\hat{i}_g(t) &= I\hat{d}_1(t) + \hat{i}(t)D_1
\end{aligned} \qquad 2.41$$

Now performing the state-space averaging technique to the second order flyback converter shown in Fig. 5a. The autonomous state variables normally are the capacitor voltage $v_c(t)$ and the inductor current i(t) which makes the state vector

$$x(t) = \begin{bmatrix} i(t) \\ v_c(t) \end{bmatrix} \qquad 2.42$$

The voltage $v_g(t)$, and the voltage across the diode drop is an independent source, which should be located in the input vector as

$$u(t) = \begin{bmatrix} v_g(t) \\ V_d \end{bmatrix} \qquad 2.43$$

In order to design the converter input and output port, we want to find the input current $i_g(t)$ and output voltage v(t) of the converter. In order to estimate this dependent current and voltage, it must be involved in the output vector y(t) as

$$y(t) = \begin{bmatrix} i_g(t) \\ v(t) \end{bmatrix} \qquad 2.44$$

Once the MOSFET is conducting and diode is off, the converter circuit of Fig. 5b is found. The capacitor current, inductor voltage, input current and output voltage of the converter are

$$C\frac{dv_c(t)}{dt} = -\frac{v_c(t)}{R+R_c} \qquad 2.45$$

$$L_m \frac{di(t)}{dt} = v_g(t) - R_{sw} i(t) \qquad 2.46$$

$$i_g(t) = i(t) \tag{2.47}$$

$$v(t) = \frac{v_c(t)R}{R+R_c} \tag{2.48}$$

After organizing the terms in (2.45)-(2.48), the result can be expressed in the subsequent state-space format

$$\begin{bmatrix} \frac{di(t)}{dt} \\ \frac{dv_c(t)}{dt} \end{bmatrix} = \begin{bmatrix} \frac{-R_{sw}}{L_m} & 0 \\ 0 & -\frac{1}{RC+R_cC} \end{bmatrix} \begin{bmatrix} i(t) \\ v_c(t) \end{bmatrix} + \begin{bmatrix} \frac{1}{L_m} & 0 \\ 0 & 0 \end{bmatrix} \begin{bmatrix} v_g(t) \\ V_d \end{bmatrix} \tag{2.49}$$

$$\begin{bmatrix} i_g(t) \\ v(t) \end{bmatrix} = \begin{bmatrix} 1 & 0 \\ 0 & \frac{R}{R+R_c} \end{bmatrix} \begin{bmatrix} i(t) \\ v_c(t) \end{bmatrix} + \begin{bmatrix} 0 & 0 \\ 0 & 0 \end{bmatrix} \begin{bmatrix} v_g(t) \\ V_d \end{bmatrix} \tag{2.50}$$

So, the state-space equations for the first subinterval have been identified.

During second subinterval, when MOSFET is not conducting and diode is on, the converter circuit of Fig. 5c is found. For the second subinterval, input current, capacitor current, output voltage, and the inductor voltage of the converter are expressed below

$$i_g(t) = 0 \tag{2.51}$$

$$C\frac{dv_c(t)}{dt} = -\frac{i(t)nR}{R-R_c} - \frac{v_c(t)}{R-R_c} \tag{2.52}$$

$$v(t) = \frac{i(t)nR_cR}{R-R_c} + \frac{v_c(t)R}{R-R_c} \tag{2.53}$$

$$L_m\frac{di(t)}{dt} = \frac{i(t)n^2R_cR}{R-R_c} + \frac{v_c(t)nR}{R-R_c} - V_dn \tag{2.54}$$

After organizing them and writing in state-space form, we get

$$\begin{bmatrix} \frac{di(t)}{dt} \\ \frac{dv_c(t)}{dt} \end{bmatrix} = \begin{bmatrix} \frac{n^2R_cR}{RL_m-R_cL_m} & \frac{nR}{RL_m-R_cL_m} \\ -\frac{nR}{RC-R_cC} & -\frac{1}{RC-R_cC} \end{bmatrix} \begin{bmatrix} i(t) \\ v_c(t) \end{bmatrix} + \begin{bmatrix} 0 & -\frac{n}{L_m} \\ 0 & 0 \end{bmatrix} \begin{bmatrix} v_g(t) \\ V_d \end{bmatrix} \tag{2.55}$$

$$\begin{bmatrix} i_g(t) \\ v(t) \end{bmatrix} = \begin{bmatrix} 0 & 0 \\ \frac{nR_cR}{R-R_c} & \frac{R}{R-R_c} \end{bmatrix} \begin{bmatrix} i(t) \\ v_c(t) \end{bmatrix} + \begin{bmatrix} 0 & 0 \\ 0 & 0 \end{bmatrix} \begin{bmatrix} v_g(t) \\ V_d \end{bmatrix} \tag{2.56}$$

So, the space-space equation of the second interval has also been identified.

The next step is to combine the result and obtain the state-space averaged model as

$$A = A_1D_1 + A_2D_2 = \begin{bmatrix} \frac{-R_{sw}}{L_m} & 0 \\ 0 & -\frac{1}{RC + R_cC} \end{bmatrix} D_1 + \begin{bmatrix} \frac{n^2R_cR}{RL_m - R_cL_m} & \frac{nR}{RL_m - R_cL_m} \\ -\frac{nR}{RC - R_cC} & -\frac{1}{RC - R_cC} \end{bmatrix} D_2$$

$$= \begin{bmatrix} \frac{-R_{sw}D_1}{L_m} + \frac{n^2R_cRD_2}{RL_m - R_cL_m} & \frac{nRD_2}{RL_m - R_cL_m} \\ -\frac{nRD_2}{RC - R_cC} & -\frac{D_1}{RC + R_cC} - \frac{D_2}{RC - R_cC} \end{bmatrix} \quad 2.57$$

$$B = B_1D_1 + B_2D_2 = \begin{bmatrix} 1 & 0 \\ L_m & \\ 0 & 0 \end{bmatrix} D_1 + \begin{bmatrix} 0 & -\frac{n}{L_m} \\ 0 & 0 \end{bmatrix} D_2 = \begin{bmatrix} \frac{D_1}{L_m} & -\frac{nD_2}{L_m} \\ 0 & 0 \end{bmatrix} \quad 2.58$$

$$C = C_1D_1 + C_2D_2 = \begin{bmatrix} 1 & 0 \\ 0 & \frac{R}{R + R_c} \end{bmatrix} D_1 + \begin{bmatrix} 0 & 0 \\ \frac{nR_cR}{R - R_c} & \frac{R}{R - R_c} \end{bmatrix} D_2$$

$$= \begin{bmatrix} D_1 & 0 \\ \frac{nR_cRD_2}{R - R_c} & \frac{RD_1}{R + R_c} + \frac{RD_2}{R - R_c} \end{bmatrix} \quad 2.59$$

$$E = E_1D_1 + E_2D_2 = \begin{bmatrix} 0 & 0 \\ 0 & 0 \end{bmatrix} D_1 + \begin{bmatrix} 0 & 0 \\ 0 & 0 \end{bmatrix} D_2 = \begin{bmatrix} 0 & 0 \\ 0 & 0 \end{bmatrix} \quad 2.60$$

Consequently, the required state-space averaged model of the flyback converter with basic parasitics in continuous conduction mode turn out to be

$$\begin{bmatrix} \frac{di(t)}{dt} \\ \frac{dv_c(t)}{dt} \end{bmatrix} = \begin{bmatrix} \frac{-R_{sw}D_1}{L_m} + \frac{n^2R_cRD_2}{RL_m - R_cL_m} & \frac{nRD_2}{RL_m - R_cL_m} \\ -\frac{nRD_2}{RC - R_cC} & -\frac{D_1}{RC + R_cC} - \frac{D_2}{RC - R_cC} \end{bmatrix} \begin{bmatrix} i(t) \\ v_c(t) \end{bmatrix}$$

$$+ \begin{bmatrix} \frac{D_1}{L_m} & -\frac{nD_2}{L_m} \\ 0 & 0 \end{bmatrix} \begin{bmatrix} v_g(t) \\ V_d \end{bmatrix} \quad 2.61$$

$$\begin{bmatrix} i_g(t) \\ v(t) \end{bmatrix} = \begin{bmatrix} D_1 & 0 \\ \frac{nR_cRD_2}{R - R_c} & \frac{RD_1}{R + R_c} + \frac{RD_2}{R - R_c} \end{bmatrix} \begin{bmatrix} i(t) \\ v_c(t) \end{bmatrix} + \begin{bmatrix} 0 & 0 \\ 0 & 0 \end{bmatrix} \begin{bmatrix} v_g(t) \\ V_d \end{bmatrix} \quad 2.62$$

The state-space averaged model has been constructed in MATLAB/Simulink. The parameters of the converter with basic parasitics in Continuous Conduction Mode are given in **APPENDIX A**.

After applying perturbation to include line voltage differences. Consequently, the variations in output and input vectors is observed, the perturbed expression get transformed as follows:

$$\begin{aligned}\dot{\tilde{x}} &= AX + BV_s + A\tilde{x} + B\tilde{v}_s \\ &+[(A_1 - A_2)X + (B_1 - B_2)V_s]\tilde{d} \\ &+[(A_1 - A_2)\tilde{x} + (B_1 - B_2)\tilde{v}_s]\tilde{d} \\ Y + \tilde{y} &= C^T X + C^T\tilde{x} + (C_1^T - C_2^T)X\tilde{d} \\ &+(C_1^T - C_2^T)\tilde{x}\tilde{d}\end{aligned} \qquad 2.63$$

On excluding the small signals in the above equation, the variation of duty ratio with respect to the state variable or output transfer functions can be directly found as:

$$\frac{\tilde{x}}{\tilde{d}} = (sI - A)^{-1}\,[\,(A_1 - A_2)\,X + (B_1 - B_2)\,V_s] \qquad 2.64$$

$$\frac{\tilde{y}}{\tilde{d}} = C(sI - A)^{-1}\,[(A_1 - A_2)\,X + (B_1 - B_2)\,V_s] + (C_1 - C_2)\,X \qquad 2.65$$

The above equation that represents the transfer function of the flyback converter will be used for studying the stability.

CHAPTER 3

3. LINEAR CONTROL SYSTEM

A controller is a device or algorithm that receives information from a measuring instrument, compares with a fixed reference value also called set point and if necessary, generates a signal to control element to take corrective measures. A controller is a tool that seeks to minimalize the difference between the actual value of the process variable and the desired value of the setpoint. Control loop is a management system to optimise a process. It measures the process value and tell us whether the process is too slow or too high. Controller may perform complex mathematical calculation to compare a set of data to a setpoint. It may also simple subtraction or addition calculations to make comparisons.

The significant uses of the controllers comprise:

a. It improves the stability of a system by stabilizing the steady state of the system.

b. By reducing the steady state error in a system, controller improvise the steady state accuracy.

c. Peak overshoot during transient condition can be controlled by a controller.

d. Any offset present in a system is minimised by a controller by changing the set point.

e. Disturbance or uncertainties introduced by some external agents is also controlled by a controller.

f. It speeds up the performance of sluggish overdamp system.

There are basic 3 modes of controller and each controller has specific advantages and limitations. They are

1. Proportional controllers.
2. Integral controllers.
3. Derivative controllers.

The combination of these controller modes used in different systems to control their stability and increase their performance. Each combination has its own advantage and limitations. They are

I. Proportional plus integral controllers (PI Controller)

II. Proportional plus derivative controllers (PD Controller)

III. Proportional plus integral plus derivative control (PID Controller)

In our project , we will be focusing only on PID controller as it is a combination of all the three mode and used very prominently in the control system.

The basic control loop topology for a single-input-single-output (SISO) system as shown in Fig. 6 . Disturbances from external agents also causes major problem in a system but here we are neglecting the disturbance.

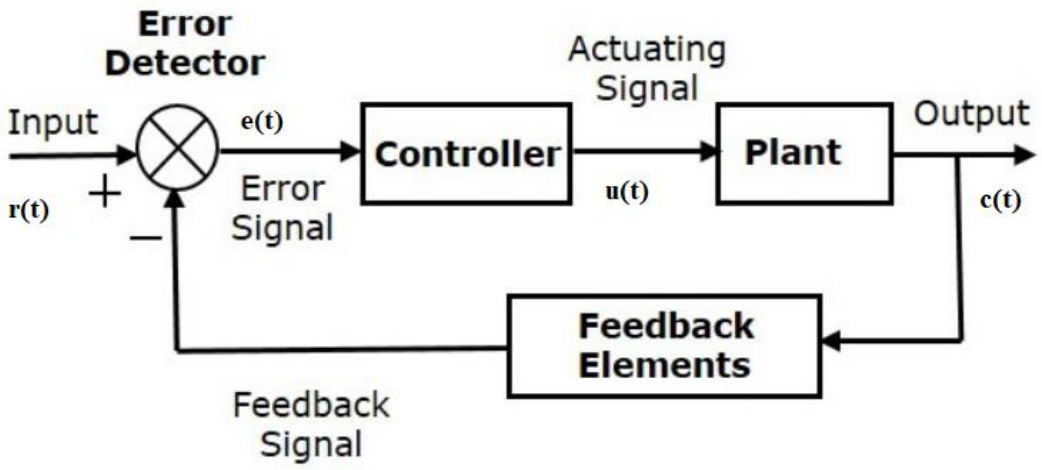

Fig. 6 : A Closed Loop SISO System

There are variety of method to design a controller in order to attain a desirable performance. Proportional controller alone operates with some residual error in a system. Still Proportional plus Integral Controller eliminates this error, but it produces oscillations and sluggish in nature. But the combination of all three modes gives best result by improving the responsiveness of a system. Almost 95% of industries use this PID controller in their system. Below equation shows the output expression for a PID controller u(t) and can be expressed in terms of the input error e(t), as:

$$u(t) = K_p \left[e(t) + \tau_d \frac{de(t)}{dt} + \frac{1}{\tau_i} \int_0^t e(\tau)\, d\tau \right] \qquad 3.1$$

and its transfer function can be written as:

$$C(s) = K_p\left(1 + \tau_d s + \frac{1}{\tau_i s}\right) \quad 3.2$$

The terms of the controller are:

K_p = Proportional gain

τ_d = Derivative time, and

τ_i = Integral time.

3.1. Proportional plus Integral plus Derivative (PID) control

Most of the desired performance of a system can be achieved by suitable combination of Proportional, Integral and Derivative control action. The P-I-D controller is widely implemented because it is easy to understand and is quite operative. The transfer function of a PID controller is expressed by:

$$C(s) = K_p\left(1 + \tau_d s + \frac{1}{\tau_i s}\right)$$

It is a second order controller, but it has versatile applicability. Any type of SISO system can use this controller, e.g. linear, nonlinear, time delay, etc. For MIMO system, it is first decoupled into many SISO system and PID controller is implemented in each SISO system. Though, for suitable implementation, a controller has to be tuned for a precise process; i.e. choice of P,I,D constraints are very important and process dependent. Unless the parameters are precisely selected, a controller may reason variability to the closed loop system.

The general variation with each controller parameter on a closed loop system is tabulated below:

CLOSE LOOP RESPONSE	RISE TIME	OVERSHOOT	SETTLING TIME	S-S ERROR
Kp	Decrease	Increase	Small Change	Decrease
Ki	Decrease	Increase	Increase	Decrease
Kd	Small Change	Decrease	Decrease	No Change

Adjust each of the gains Kp, Ki and Kd until you obtain a desired overall response.

It is not always essential that all the combination of proportional, derivative and integral actions should be combined in the controller. In most of the cases, a simple P-I assembly will aid the objective. This thesis also deals with the PID controller implementation on flyback converter in subsequent section for comparative study.

CHAPTER 4

4. DISCRETE MODELLING OF FLYBACK CONVERTER

Some difficulties are faced in the analysis of both the electrical networks and power electronic circuits. Considering this, it is more suitable and elegant in switching circuits, to opt for the modified nodal analysis (MNA) method. To further facilitate the analysis, system equations can be obtained with MNA using discrete circuit models known as companion models. The companion (or discrete) circuit model transforms the system containing dynamic elements into a fully resistive analysis. In discrete model, there is no need to use differential equations. The main contribution of this topic is that it proposes an efficient analysis method for power electronics circuits containing coupled inductors. The method transforms any dynamic circuit into resistive circuit.

In this chapter firstly, discrete modelling with coupled (or mutual) inductors. The fully discrete model of the flyback converter using the proposed model is represented.

4.1. DISCRETE MODELLING OF COUPLED INDUCTOR AND CAPACITOR

Circuits with coupled inductors can interact with each other in pairs, triples or more. Mutual inductance positively or negatively affects the voltages to be induced according to the positions of windings in the coils. Coupled inductor is widely used in all kinds of power electronics circuits where multiple output selection, ripple reduction, snubber option, electrical isolation etc. are required. The model of the circuit with mutual inductances, which has double interaction, is shown in Figure 1 and the related circuit equations (or terminal equations of coupled inductors) are given in Eqs. (4.1) and (4.2).

$$V_1 = L_1 \frac{di1}{dt} - m \frac{di2}{dt} \qquad 4.1$$

$$V_2 = L_2 \frac{di2}{dt} - \mathrm{m} \frac{di2}{dt} \quad 4.2$$

We get discrete model, by comparing above equations with the equation mentioned below in order to be solved by any numerical integration, Backward Euler integration method is used for analysis

$$\frac{dx}{dt} = f(x) \quad 4.3$$

$$x_{(n+1)} = x_n + \mathrm{hf}(x_{n+1}, t_{n+1}) \quad 4.4$$

By applying the integration formula to the to the pair of mutual inductors, the corresponding discrete model is obtained.

$$i_{1(n+1)} = i_{1n} + \frac{hL_2}{L_1L_2 - m^2} V_{1(n+1)} + \frac{hm}{L_1L_2 - m^2} V_{2(n+1)} \quad 4.5$$

$$i_{2(n+1)} = i_{2n} + \frac{hL_1}{L_1L_2 - m^2} V_{2(n+1)} + \frac{hm}{L_1L_2 - m^2} V_{1(n+1)} \quad 4.6$$

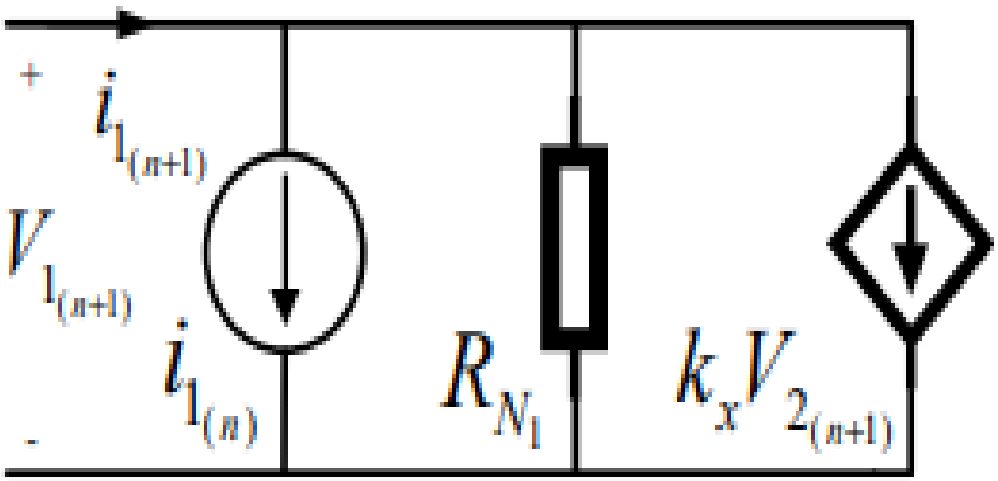

Figure 7. Discrete model of primary side inductor

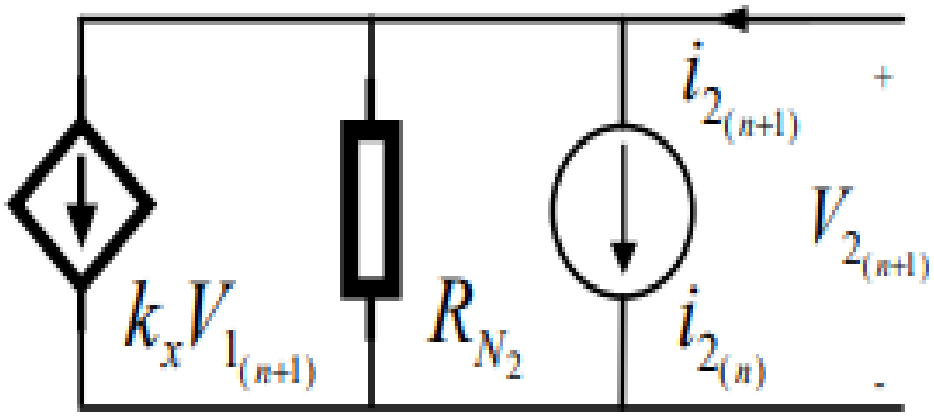

Figure 8. Discrete model of secondary side inductor

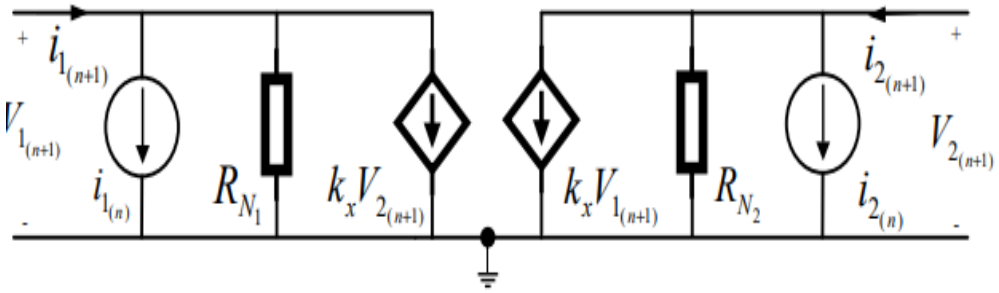

Figure 9. Discrete model of fully coupled inductor

$$R_{N1} = \frac{L_1 L_2 - M^2}{hL_2} \quad 4.7$$

$$R_{N2} = \frac{L_1 L_2 - M^2}{hL_1} \quad 4.8$$

$$K = \frac{hM}{L_P L_S - M^2} \quad 4.9$$

Similarly, equations and equivalent circuit for the discrete model of a capacitor is as follows

$$i_{n+1} = \frac{c}{h} V_{n+1} - \frac{c}{h} V_n \quad 4.10$$

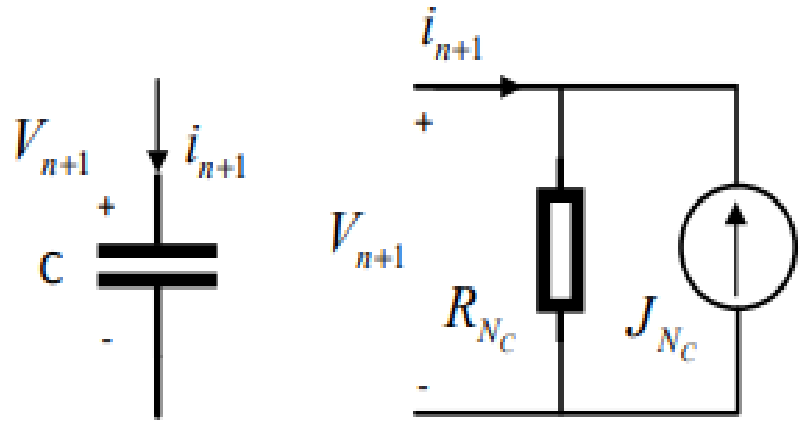

Figure 10. Discrete model of Capacitor

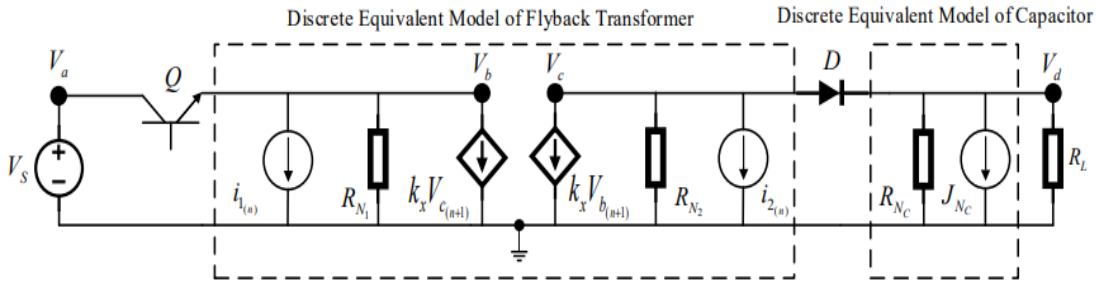

Figure 11.. Discrete Equivalent Circuit of Flyback Converter

By using the discrete equivalent model of the coupled inductors instead of the high frequency flyback transformer and the companion model instead of the capacitor, the system is free of inductance and capacitance and this process makes it completely resistive.

The MNA approach is used to obtain the system equations. The general structure of the MNA method in the time domain is expressed in Equation.

$$x(t) = G^{-1} B\, u(t) \qquad 4.11$$

Where

G: Conductance Matrix

B: Constant Matrix

x(t): Column Matrix of unknown node voltages & currents

u(t): Column matrix of known independent sources

$$x(t) = [\, V_a\ V_b\ V_c\ V_d\ I_{vs}\ I_{vx}]^{-1} \qquad 4.12$$

$$u(t) = [\, V_s\ V_x\ i_{1n}\ i_{2n}\ J_x\ J_{Nc}]^{-1} \qquad 4.13$$

Two-valued element or ideal switch approach can be used in modelling semiconductor switching elements. While there is only one topology in the two-valued element

approach, in the case of the ideal switch, the circuit topology varies depending on the positions of the switches. Also, the switches can be modelled with an independent voltage source in the on state and with independent current sources in the off-state, with their values being zero. In this chapter, the semiconductor switch Q. and the semiconductor power diode, D, are modelled with the independent voltage and current source approach. In Position I, Q switch is on and D diode is off. In Position II, Q switch is off and D diode is on.

During Ton

At node a

$$I_{vs} = -I_{vx} \quad 4.14$$
$$V_a - V_b = V_x \quad 4.15$$
$$V_s = V_a \quad 4.16$$

At node b

$$-I_{vx} + \frac{V_b}{R_{N1}} + K_x V_{c(n+1)} = -i_{1n} \quad 4.17$$

At node c

$$G_{N2} V_c + K_x V_{b(n+1)} = -J_x - i_{2n} \quad 4.18$$

At node d

$$(G_{Nc} + G_l) V_d = J_x + J_{Nc} \quad 4.19$$

During Toff

At node a

$$I_{vs} + J_x = 0 \quad 4.20$$

At node b

$$\frac{V_b}{R_{N1}} + K_x V_{c(n+1)} = -i_{1n} + J_x \quad 4.21$$

At node c

$$G_{N2} V_c + K_x V_{b(n+1)} + I_{vx} = -i_{2n} \quad 4.22$$

At node d

$$(G_{Nc} + G_l) V_d - I_{vx} = -J_{Nc} \quad 4.23$$

These nodal equations provide us with the matrices we require in MNA Approach i.e. providing us conductance and constant matrices.

$$G_1 = \begin{bmatrix} 0 & 0 & 0 & 0 & 1 & 1 \\ 0 & G_{N_1} & k_x & 0 & 0 & -1 \\ 0 & k_x & G_{N_2} & 0 & 0 & 0 \\ 0 & 0 & 0 & G_{N_C} + G_L & 0 & 0 \\ 1 & 0 & 0 & 0 & 0 & 0 \\ 1 & -1 & 0 & 0 & 0 & 0 \end{bmatrix} \quad 4.24$$

$$G_2 = \begin{bmatrix} 0 & 0 & 0 & 0 & 1 & 0 \\ 0 & G_{N_1} & k_x & 0 & 0 & 0 \\ 0 & k_x & G_{N_2} & 0 & 0 & 1 \\ 0 & 0 & 0 & G_{N_C} + G_L & 0 & -1 \\ 1 & 0 & 0 & 0 & 0 & 0 \\ 0 & 0 & 1 & -1 & 0 & 0 \end{bmatrix} \quad 4.25$$

$$B_1 = \begin{bmatrix} 0 & 0 & 0 & 0 & 0 & 0 \\ 0 & 0 & -1 & 0 & 0 & 0 \\ 0 & 0 & 0 & -1 & -1 & 0 \\ 0 & 0 & 0 & 0 & 1 & 1 \\ 1 & 0 & 0 & 0 & 0 & 0 \\ 0 & 1 & 0 & 0 & 0 & 0 \end{bmatrix} \quad 4.26$$

$$B_2 = \begin{bmatrix} 0 & 0 & 0 & 0 & -1 & 0 \\ 0 & 0 & -1 & 0 & 1 & 0 \\ 0 & 0 & 0 & -1 & 0 & 0 \\ 0 & 0 & 0 & 0 & 0 & 1 \\ 1 & 0 & 0 & 0 & 0 & 0 \\ 0 & 1 & 0 & 0 & 0 & 0 \end{bmatrix} \quad 4.27$$

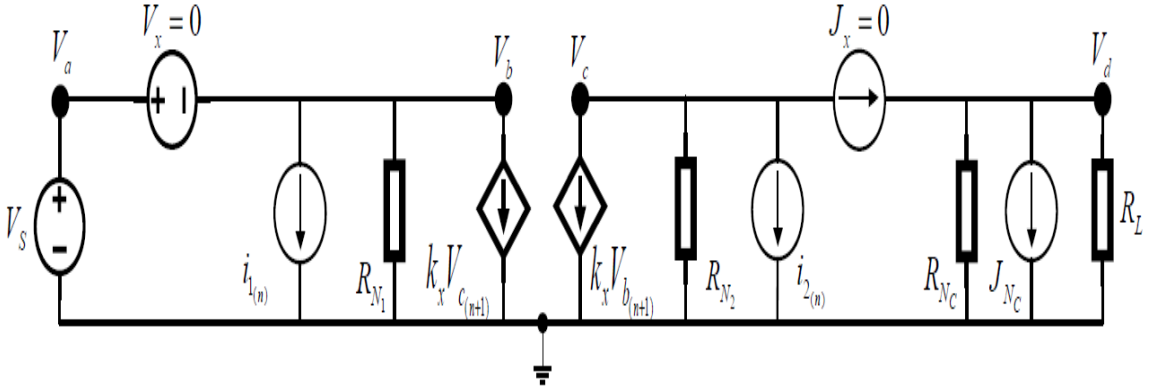

Figure 12. Circuit Topology for ON State

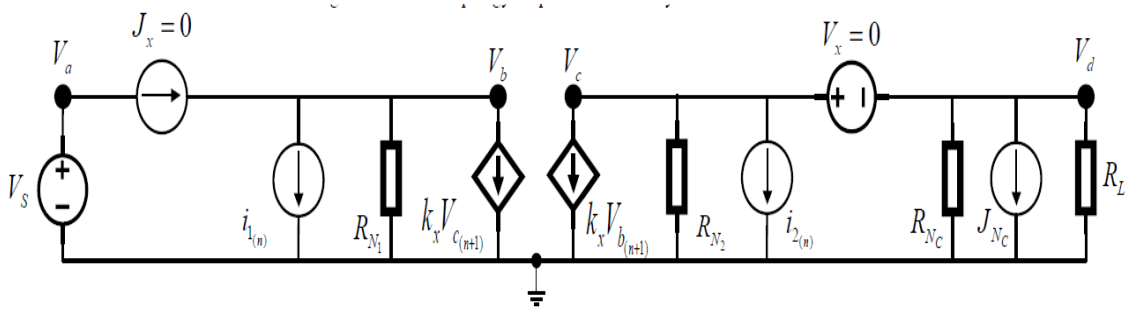

Figure 13. Circuit Topology for OFF State

CHAPTER 5

5. FLYBACK CONVERTER DESIGN

5.1. INSPIRATION

Flyback converter can be seen in most of the applications in consumer products as compared to other switching converter topologies. Both non isolated and isolated converters are equally popular in commercial applications like computer's SMPS, laptops, mobile charger, DC drives and other domestic and office equipment's etc. Still isolated switching converters are chosen where load protection, multiple output, decrease noise interference etc. It is beneficial in the system where step up, step down polarity reversal operation is required.

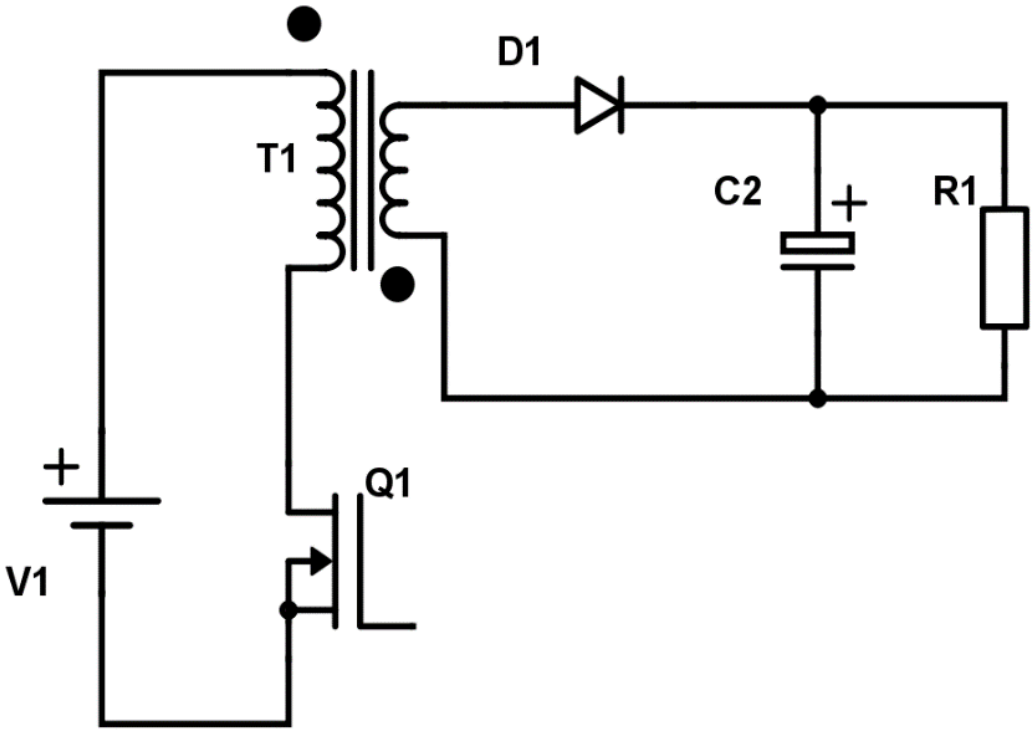

Fig. 14 : Flyback Converter Topology.

5.1.1. DESIGN SPECIFICATION

V_{in}: 220 VAC

V_{out}: 5 V, 2 A $(secondary\ winding)$

f_s: 100 kHz

5.1.2. CONTINOUS CONDUCTION MODE

Conduction mode in power converters refer to whether the current in the energy storage element goes to zero during each switching cycle or not. We start with the design of flyback converter let us assume N1: N2 = 320: 6 and D = 0.5 as a initialization for Continuous Conduction mode using law of energy conservation for one cycle,

$$P_{out}(\ transformer\ ) = P(\ diode\ ) + P(\ load\ )$$

$$(V_{out} + 1) * \frac{I_{s_{peak}}}{2} * (1 - D) = V_D * \frac{I_{s_{peak}}}{2} * (1 - D) + V_{out} * I_{out} \quad 5.1$$

$$6 * \frac{I_{s_{peak}}}{2} * 0.5 = 1 * \frac{I_{s_{peak}}}{2} * 0.50 + 5*2 \quad 5.2$$

$$I_{s_{peak}} = 8A \quad 5.3$$

Peak value of secondary current calculated form the above equation found out to be 8 A. With a 10% of ripple in current in magnetic inductance. From this we can deduce that value of inductance as,

$$\frac{V_{out}+1}{L} * (1 - D) * T = \frac{10}{100} * 8 \quad 5.4$$

$$L = 1.5MH \quad 5.5$$

1.5 MH of inductance will make the dimensions of transformer of converter large. As size and weight in converter matters the most. Hence, we cannot continue with this design in Continuous Conduction Mode (CCM).

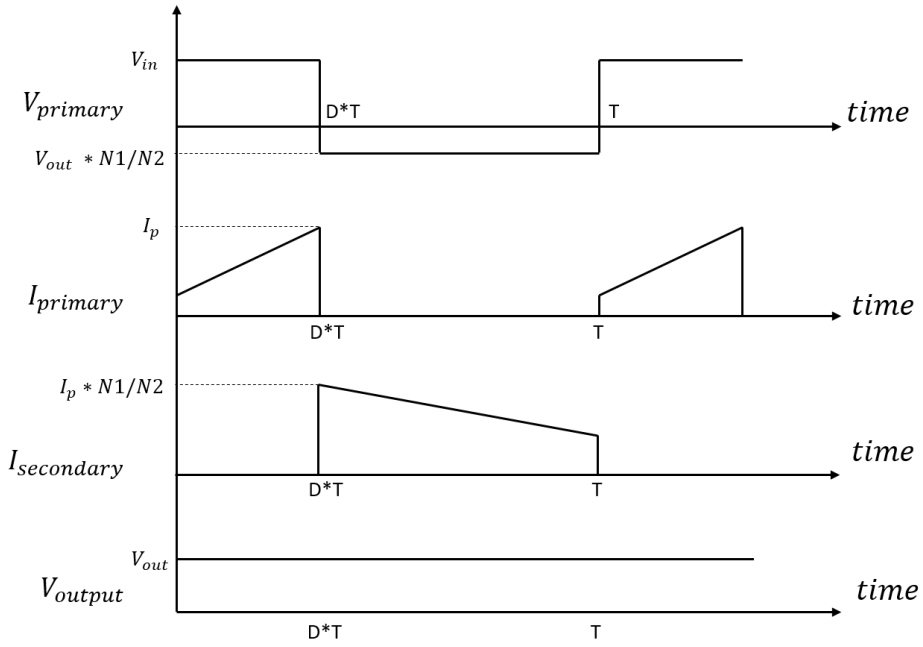

Fig. 15 : Current and Voltage waveform under CCM for Flyback Converter.

5.1.3. DISCONTINOUS CONDUCTION MODE

In Discontinuous Conduction Mode (DCM) all the energy in every period is consumed and the magnetising inductor stays with no current and no stored energy for small span of time. Given the high value of magnetizing inductance got in CCM, considering a value such 1mH as right value for magnetizing inductance in DCM. As in Discontinuous Conduction Mode, the switching current always starts from zero which means no stored energy, so this is a low dissipating switching transition which is beneficial for good efficiency and EMI. Keeping same values for the turn's ratio with all consideration of drop across the diode (i.e.1V).

From equation $V = L\frac{di}{dt}$ we find,

$$\frac{V_p}{L_p} * D * T = Ip_{peak} \qquad 5.6$$

V_p : $Primary\ side\ voltage$

D: $Duty\ cycle$

L_p: $Primary\ side\ magnetizing\ inductance$

Ip_{peak}: $Primary\ current\ peak\ value$

And from law of conservation of energy we found,

$$V_p * \frac{Ip_{peak}}{2} * D = 5 * 2 \qquad 5.7$$

Dividing two equations (5.6) and (5.7), the value of peak secondary current is found to be,

$$Ip_{peak} \approx 0.45\ A \qquad 5.8$$

Value of Ip_{peak} can be substituted in any of the two equations to get the value of duty cycle which is,

$$D = 0.1406 \qquad 5.9$$

Fig. 16 represents waveforms for DCM operation at steady state.

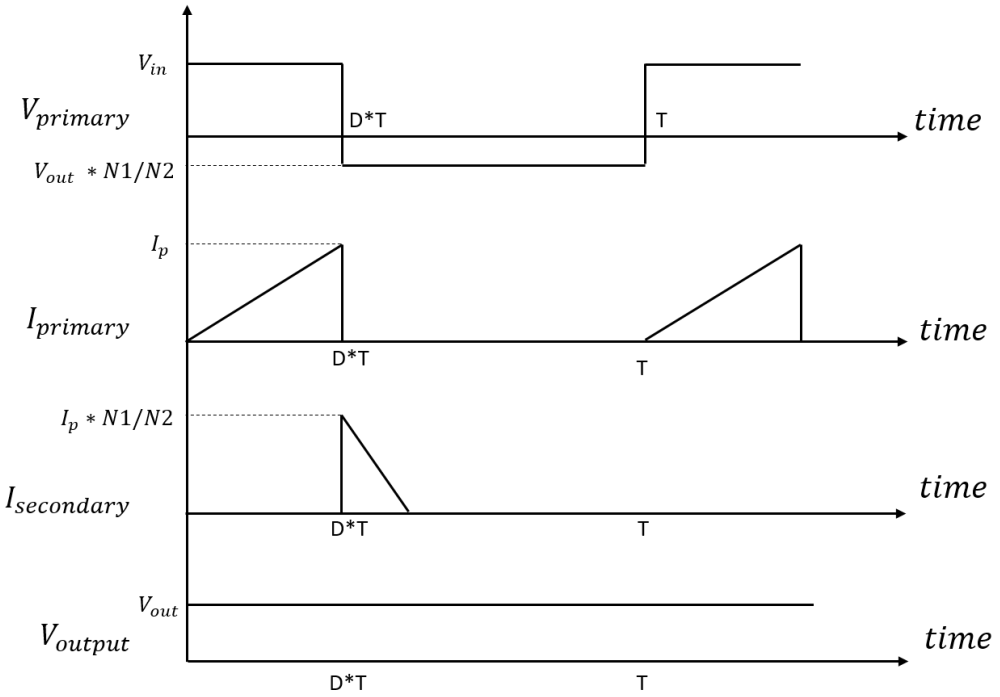

Fig. 16 : Current and Voltage waveform under DCM for Flyback Converter.

Taking consideration of 1%ripple in output voltage capacitor value is calculated. Considering that the duty ratio which is obtained in the above equation is applicable for full load condition only. So, a closed loop control is necessary as feedback.

CHAPTER 6

6. TESTING AND RESULT

The transfer functions given by equations (2.64) and (2.65) are considering the parasitic values and all components of the circuit. Below flowchart shown in plot, the steps while coding the model for flyback converter.

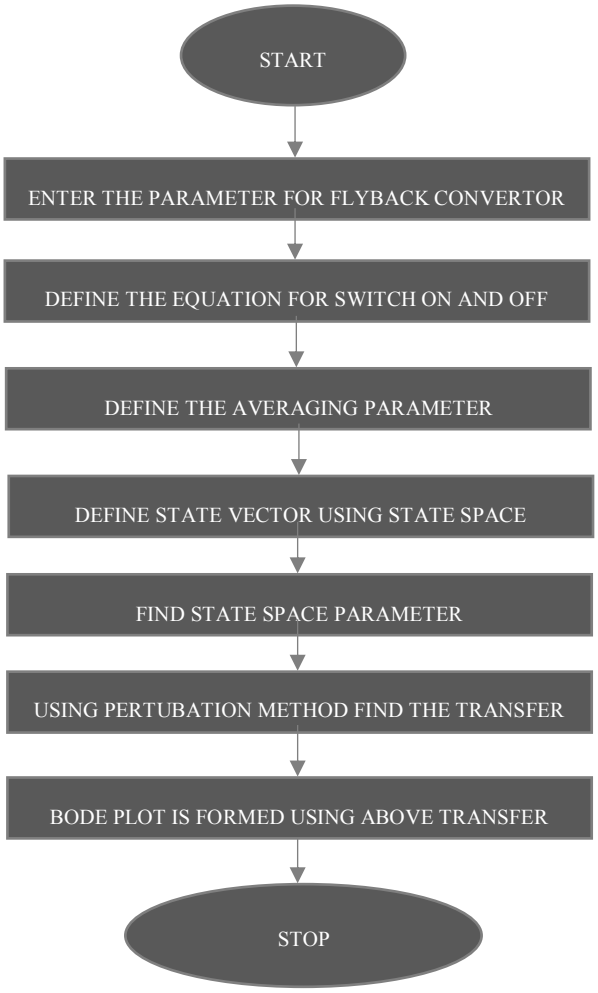

Fig. 17 : Flowchart to design bode plot.

To study the stability and modelling for flyback converter, the parameters for the converter as written in **APPENDIX A** is entered in the m-file of MATLAB. The exact value for the model with all notation is entered to find the transfer function of the model. As soon as the parameters are defined, equation for switch ON/OFF condition are defined with their differential equation. With this step averaging parameters are defined to design the state vector using state space averaging technique.

Lastly using perturbation method transfer functions are derived from the state vectors. With this transfer function bode plot is developed and stability is studied.

The following assumptions are made while designing:

(i) R_c is very small when compared with R. Therefore, neglect it.

(ii) V_d is also small compared to $v_s(t)$. Thus, neglecting V_d.

By making these assumptions in the matrices, with the specifications as given in **APPENDIX A** and using MATLAB Code as in **APPENDIX B** obtained Bode plots are as follows:

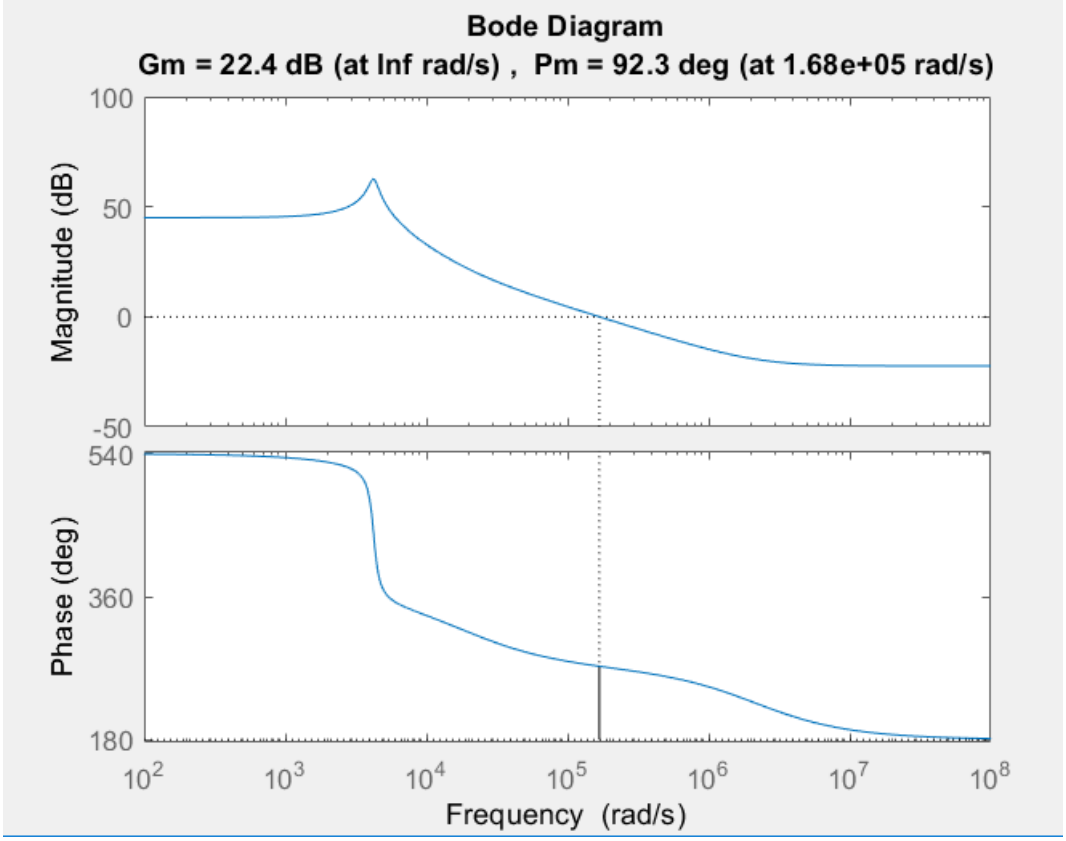

Fig. 18 : Bode Plot for the designed Flyback convertor.

The gain margin and phase margin of the designed flyback converter are tabulated below saying the system is stable as shown in Fig. 18.

Gain margin	**Phase margin**	**Stability condition**
22.4 dB	92.3^{o}	Stable

An accurate model of the flyback converter in the presence of parasitic elements is achieved. It is clear in the above table that the model designed is stable.

6.1. SIMULATION FOR PI CONTROL MODEL FOR FLYBACK CONVERTER

Simulation model designed for the flyback converter is simulated in Simulink of MATLAB under different load conditon to study its performance. Fig. 19 shows the Single output flyback converter with closed loop control using PI control algorithm in Simulink. The reason behind using PI controller is its application to different processes and its simple structure. A source of 220V is first rectifed and then fed to the input side of converter and a closed loop PID control is performed with its output of 5 Volt as a reference voltage. Proper tuning of the PID controller requires wide trials. PID block parameters like K_p, K_i and K_d are choosen after repetative trial and error method. With the value of 1, 15 and 0 for K_p, K_i and K_d respectively are entered in the PID block. Initially voltage error is given to the PID controller, then error generated is forwarded to a PWM generator for generating switching pulse for the MOSFET switch. An input current which is shown in Fig.20 during stedy state verify its performance parameter. After all the calculation for the flyback transformer and parameter for converter, performance of flyback converter is studied for closed loop PID controller. The model is simulated on MATLAB SIMULINK and various outputs are studied and verified. The parameters for Flyback Converter is shown in **APPENDIX A.**

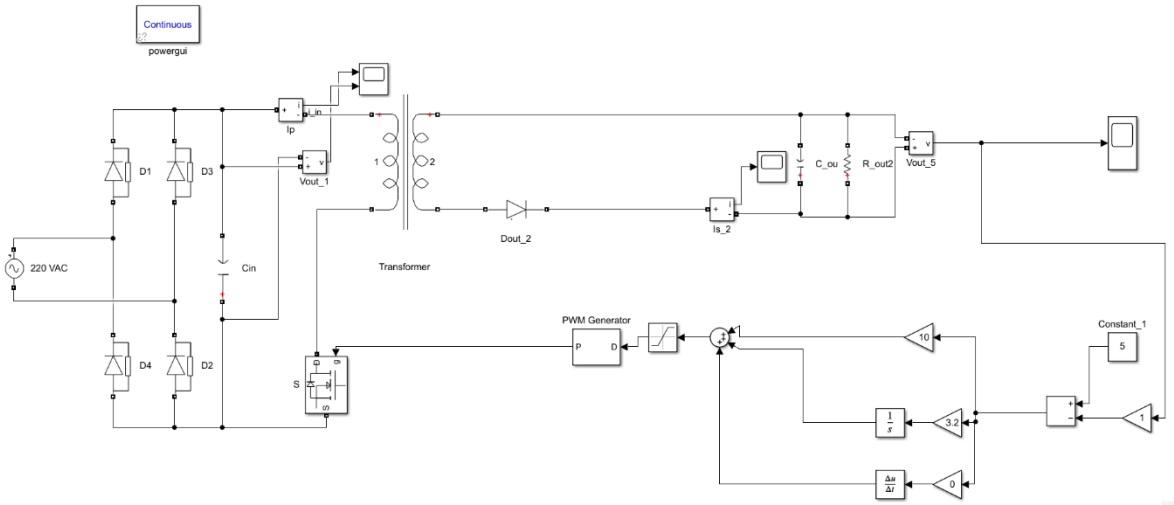

Fig. 19 : Flyback converter with closed loop control in MATLAB.

6.1.1. RESULT

After completing Simulink model in MATLAB, it is simulated to study the result.

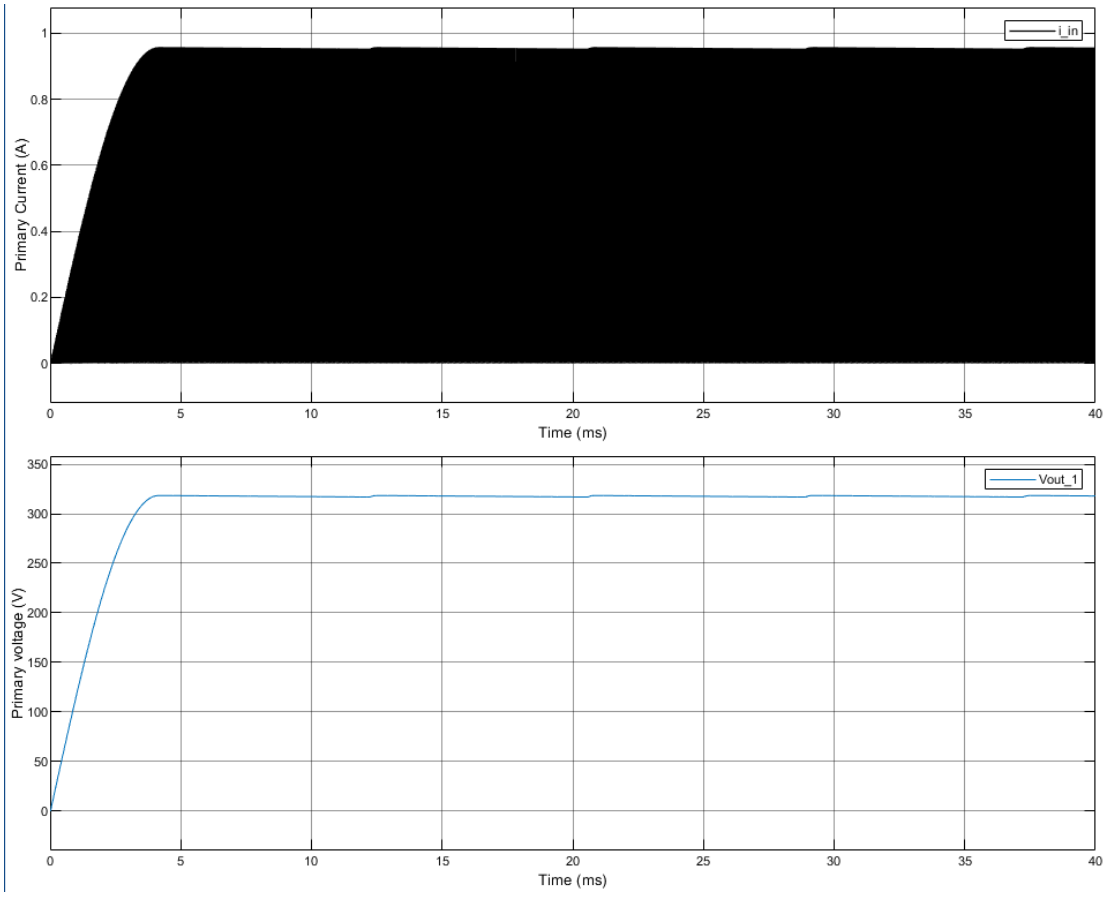

Figure 20. Primary Current and Voltage Waveform

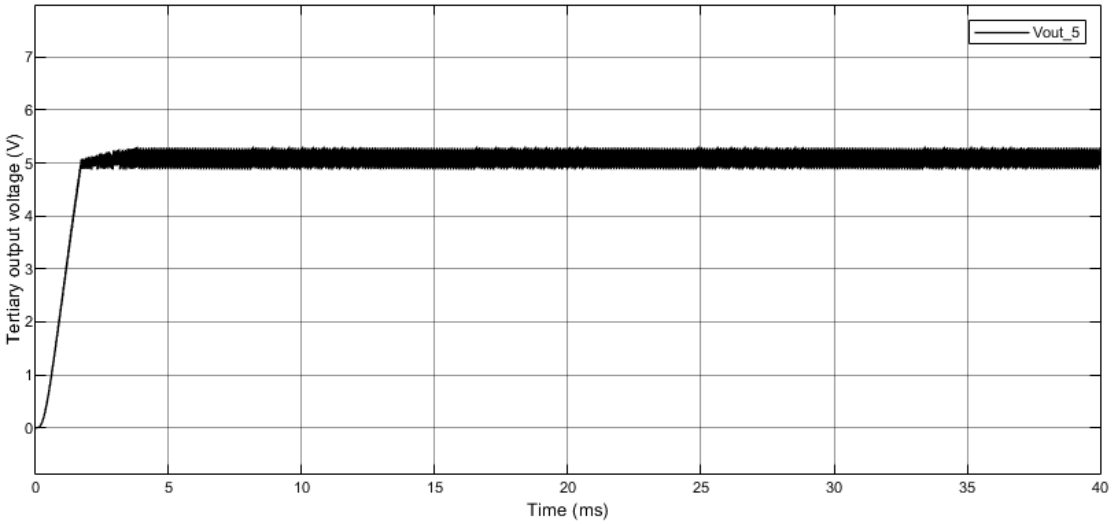

Figure 21. Controlled Output of 5V of Flyback Converter

Input current through switch is shown in figure for the designed simulation model for Flyback Converter.

CHAPTER 7

7. APPLICATION

A Modular Multilevel Converter (MMC) is one of the modern multilevel converters used for high and medium voltage power conversion. The module capacitors need to be pre-charged, to power the control circuit. If a flyback converter is used to produce the power supply for driving the control circuit, the module capacitor voltages are fetching unstable during pre-charging. It is based on cascade connection of multiple undistinguishable modules using IGBTs as switching devices. In each MMC module, the control circuit, entailing of gate drivers, is powered from a dc supply derived from the local capacitor. It is shown former that the reason for this is approximately constant power load on the module capacitor. This project demonstrates by simulation that, if the load on the module capacitor is made positive resistance load, power supply can be made stable. It shows by simulation that, even if the load on module capacitor is approximately constant power and all the power supplies are not stabilized initially, by switching devices in those modules where power supply becomes available first, followed by sorting algorithm, stable power supplies can be developed on all the modules and the capacitors can be fully charged to the desired voltage. Functional diagram of a three phase MMC is illustrated in figure.

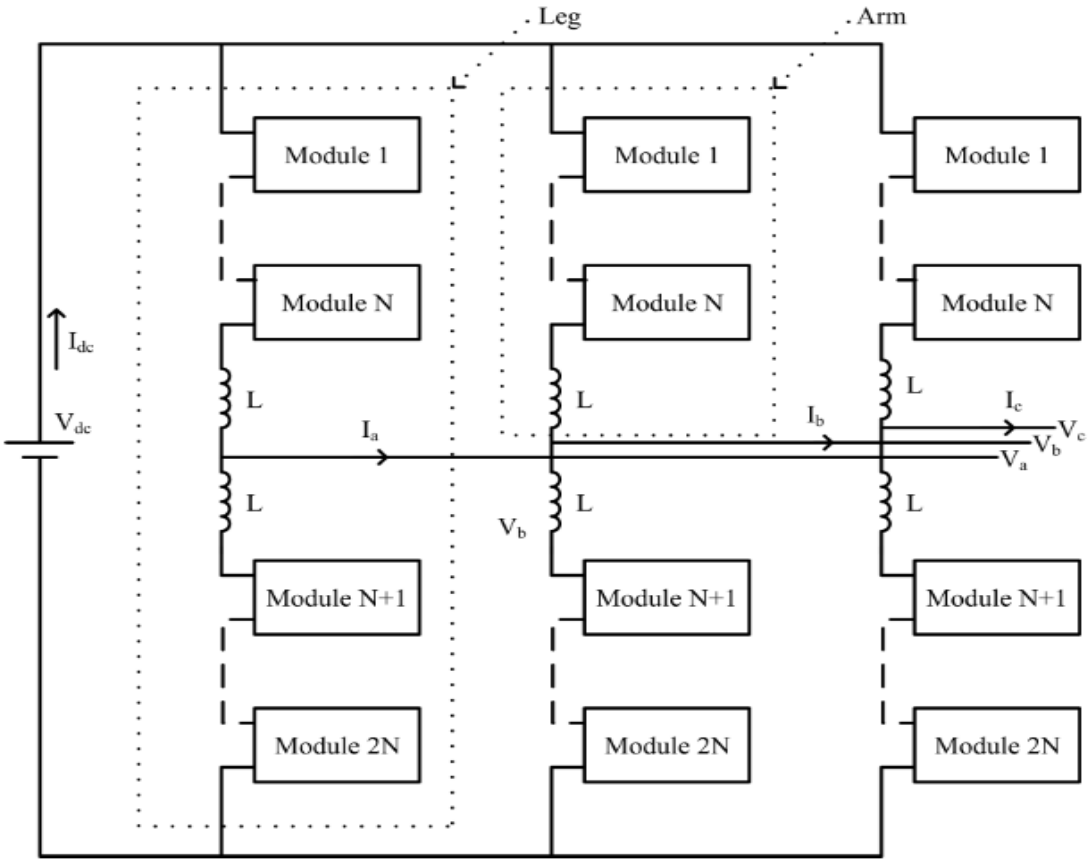

Fig. 22 : MMC for Three phase.

7.1. PRE-CHARGING MODULE CAPACITOR

A modular multilevel converter (MMC) is made up of a series connection of multiple half or full-bridge modules. It has three legs connected in parallel to a dc source. Each of these legs is made of two arms. An arm consists of a string of modules and an inductor connected in series. A half-bridge MMC module is shown in Fig. 23. The modules will allow the capacitor to be either bypassed or inserted into the arm. Half bridge module can produce two voltage levels (0 and Vc) across its terminals. where Vc is the voltage across the capacitor C. Pre-charging of its module capacitor is the main challenge associated with Modular Multilevel Capacitor. Additional power supply makes the procedure unwieldly and costly. Therefore, it is the needed to pre-charge the module capacitor with the key power supply. It is attained in two phase: in the start, an uncontrolled pre-charging of module capacitors is started through diodes of MOSFET existing in series with capacitor. Later a certain threshold voltage is attained, module capacitor output is attached with Flyback converter are employed for measured pre-

charging using sorting algorithm. Flyback converter was selected for this low power application because of its necessity for a smaller number of components.

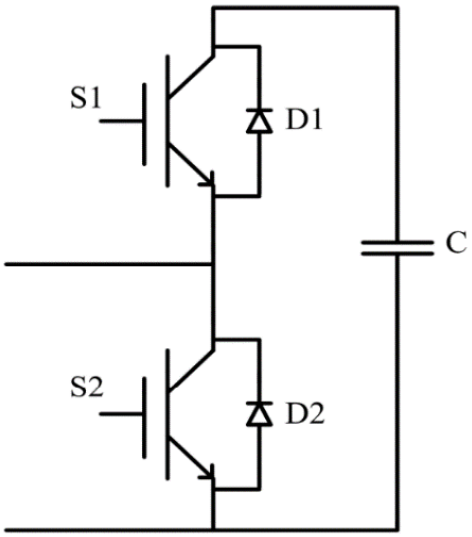

Fig. 23 : MMC with Half bridge cell.

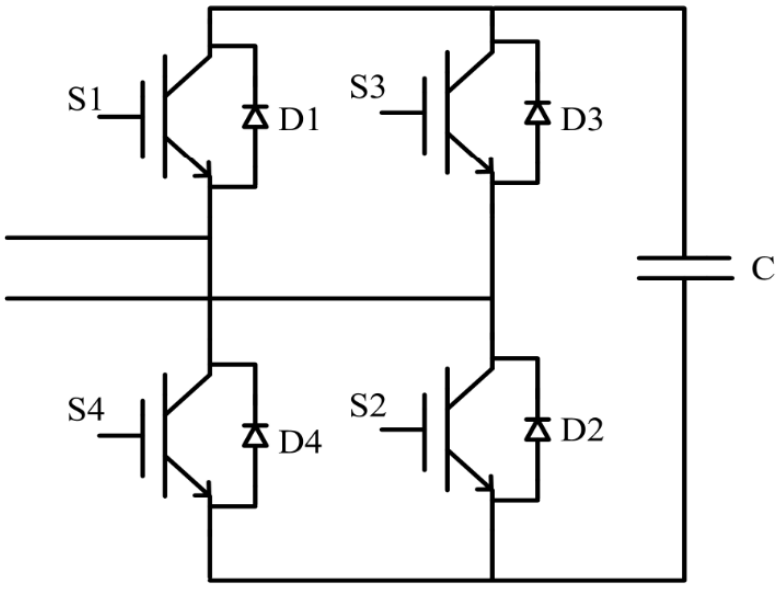

Fig. 24 : MMC with Full bridge cell.

CHAPTER 8

8. CONCLUSION

For DC/DC converter as in my case Flyback Converter, was controlled using PID Controller. This project gives methodology to model flyback converter by using state space averaging technique which linearizes the system and simplifies the design procedure. Another method based on MNA approach is also considered to model flyback converter, which transforms any dynamic circuit into resistive circuit by considering separate companion models for the coupled inductor and capacitor present in the flyback converter. This method provides us with discrete model of the flyback converter which makes the analysis easier and further provides us with opportunity to go for different controllers. Analysis in the discrete model proposed in the project is carried out with the help of MNA equations. Flyback Converter was simulated in Simulink with PID Controller for increased performance and efficiency of converter.

APPENDICES

APPENDIX A

Parameters for Flyback Converter:

V_g = 310 V

V_c = 5 V

MOSFET 4.2A, 700V

R_{sw} = 0.04 Ω

F_s = 100KHz

D_1 = 0.1406

L_m = 1mH

n = 1/62

Diode 400V, 2A

V_d = 1.25V

C = 200 μF

R = 2.5 Ω

R_c = 0.09 Ω

APPENDIX B

```
Vg = 310;
Ilm = 0.5;
Vc = 5;
I = eye(2);
X = [Ilm Vc]';
Rsw = 0.1;
Fs = 100000;
d1 = 0.1406;
d2 = 1-d1;
Css = 470*10^(-9);
Rss = 10;
Lm = 1*10^(-3);
Lp = 0.2*10^(-6);
Ls = 0.8*10^(-6);
n = 1/62;
Vd = 1;
Cds = 100*10^(-12);
Rds = 200;
C = 200*10^(-6);
Rc = 0.09;
R = 2.5;
A1 =  [-Rsw/Lm    0;
        0   -1/(R*C+Rc*C)];
A2 = [(n^2)*Rc*R/(R*Lm-Rc*Lm) n*R/(R*Lm-Rc*Lm);
      -n*R/(R*C+Rc*C) -1/(R*C+Rc*C)];
B1 = [ 1/Lm 0]';
B2 = [ 0 -n/Lm]';
C1 = [0 R/(R + Rc)];
C2 = [n*R*Rc/(R - Rc)  R/(R - Rc)];
D1 = [0];
D2 = [0];
```

```
A = (A1 * d1)+(A2 * d2);
B = (B1 * d1)+(B2 * d2);
C = (C1 * d1)+(C2 * d2);
D = (D1 * d1)+(D2 * d2);
SS= ss(A,B,C,D);
s = tf('s');
[P,Q]=ss2tf(A,B,C,D);
X1 = inv((s*I) - A)*[(A1 - A2)*X+(B1 - B2)* Vg];
Y = C*inv((s*I) - A)*[(A1 - A2)*X+(B1 - B2)*Vg]+(C1 - C2)* X;
Fig.(1);
bodeplot(Y);
margin(Y);
```

REFERENCES

[1] T. Suntio, "*Average and Small-Signal Modelling of Self-Oscillating Flyback Converter with Applied Switching Delay"*, in IEEE Transactions on Power Electronics, VOL. 21, NO. 2, March 2006.

[2] B. Singh and G.D. Chaturvedi, "*Analysis, Design and Development of a Single Switch Flyback Buck-Boost AC-DC Converter for Low Power Battery Charging Applications"*, in Journal of Power Electronics, Vol. 7, No. 4, October 2007.

[3] H. Kewei, L. Jie, F. Ningjun, L. Yuebin, H. Xiaolin, and W. Luo, "*Modelling analysis and simulation of high-voltage flyback dc-dc converter,"* in *Industrial Electronics, 2009. ISIE 2009. IEEE International Symposium on*. IEEE, July 2009, pp. 813 –818.

[4] P. Chetty, "*Current injected equivalent circuit approach to modelling switching dc-dc converters*," *Aerospace and Electronic Systems, IEEE Transactions on*, vol. AES-17, no. 6, pp. 501 –505, Nov. 1981.

[5] A. Davoudi, J. Jatskevich, and T. De Rybel, "*Numerical state-space average-value modelling of PWM dc-dc converters operating in DCM and CCM*," Power Electronics, IEEE Transactions on, vol. 21, no. 4, pp. 1003 – 1012.

[6] S. Cúk and R. Middlebrook, "*A general unified approach to modelling switching dc to dc converters in discontinuous conduction mode*," in Proc. IEEE PESC'77, 1977, pp. 36–57.

[7] D. Czarkowski and M. Kazimierczuk, "*Linear circuit models of pwm flyback and buck/boost converters*," Circuits and Systems I: Fundamental Theory and Applications, IEEE Transactions on, vol. 39, no. 8, pp. 688 –693, Aug 1992.

[8] V. Vorperian, "*Simplified analysis of PWM converters using model of PWM switch Part I: Continuous conduction mode, Part II: Discontinuous conduction mode,"* IEEE Trans. Aerospace Electron. Syst., vol. 26, May 1990, pp. 490–505.

[9] N. Mohan, T. Undeland, and W. Robbins, *Power electronics*. Wiley New York, 1995.

[10] M. H. Rashid, *Power Electronics: Circuit, Devices and Applications*, 2nd ed. Englewood Cliffs, NJ: Prentice-Hall, 1993.

[11] Seddik Bacha, Iulian Munteanu, Antoneta Iuliana Bratcu, "*Power Electronic Converters Modelling and Control with Case Studies*", Springer.

[12] Chung-Wen Ho, A. Ruehli and P. Brennan, "The modified nodal approach to network analysis," in IEEE Transactions on Circuits and Systems, vol. 22, no. 6, June 1975, pp. 504-509.

[13] H. Garcia and M. Madrigal, "Companion harmonic circuit models for transient studies", *Electr. Eng.*, vol. 95, no. 1,2013, pp. 43-51.

[14] B. Canol and A. B. Yıldız, "Discrete-Model Based Analysis of Flyback Converter Circuit," 2021 5th International Symposium on Multidisciplinary Studies and Innovative Technologies (ISMSIT), 2021, pp. 346-350.